ELSEVIER

Physica A 239 (1997) 542–601

PHYSICA A

Graphical representations and cluster algorithms I. Discrete spin systems[1]

L. Chayes[a,*], J. Machta[b]

[a] *Department of Mathematics, University of California, Los Angeles, CA 90024, USA*
[b] *Department of Physics and Astronomy, University of Massachusetts, Amherst, USA*

Received 12 July 1996; revised 21 October 1996

Abstract

Graphical representations similar to the FK representation are developed for a variety of spin-systems. In several cases, it is established that these representations have (FKG) monotonicity properties which enables characterization theorems for the uniqueness phase and the low-temperature phase of the spin system. Certain systems with intermediate phases and/or first-order transitions are also described in terms of the percolation properties of the representations. In all cases, these representations lead, in a natural fashion, to Swendsen–Wang-type algorithms. Hence, at least in the above-mentioned instances, these algorithms realize the program described by Kandel and Domany, Phys. Rev. B 43 (1991) 8539–8548. All of the algorithms are shown to satisfy a Li–Sokal bound which (at least for systems with a divergent specific heat) implies critical slowing down. However, the representations also give rise to invaded cluster algorithms which may allow for the rapid simulation of some of these systems at their transition points.

Keywords: Graphical representations; FK representation; Swendsen–Wang algorithm; Invaded cluster algorithm; Ashkin–Teller model; Cubic models; Percolation transitions; First-order transitions; Li–Sokal bounds

1. Introduction

Progress in the area of statistical mechanics, both theoretical and computational, is often achieved by means of graphical representations; the history of this subject constitutes a substantial fraction of the larger story. An exciting development that has taken place in the last few years has been introduction of cluster methods, in particular those of Swendsen and Wang [2] which facilitate the rapid computation of equilibrium ensembles.

* Corresponding author. Fax: +1 310 206 6673; e-mail; lchayes@math.ucla.edu.

[1] Work supported in part by the NSF under the grants DMS-93-02023 (L.C.) and DMR-93-11580 (J.M.).

PII S0378-4371(96)00438-4

In their original versions, these algorithms were designed for the simulation of the q-state Potts models in direct conjunction with the Fortuin and Kasteleyn representation of these systems. Even in the more advanced versions [3,4,1], the vestiges of an underlying graphical representation are present. Although these algorithms have demonstrated a considerable improvement over the traditional single-spin update methods it seems that in general they do not overcome the problem of critical slowing down. In particular, if the specific heat is divergent, then for the algorithms introduced in [2] – the SW algorithms – this is the subject of a rigorous theorem [5]:

$$\tau_{sw} \geqslant [\text{const.}] C_H \tag{1.1}$$

where τ_{sw} is the autocorrelation time and C_H is the specific heat. (In the language of critical exponents, this reads "$z \geqslant \alpha/\nu$".) It also appears that in general, the algorithms introduced in [3] experience critical slowing [6]. What is more, these problems occur on top of the need for prior knowledge or extensive pre-computation of the critical temperature.

This set of difficulties has apparently been reduced (and in certain cases appears to have been alleviated altogether) by the invaded cluster (IC) algorithm [7,8]. In addition, this algorithm provides a distinctive signal whenever the transition is discontinuous. The development of the IC algorithm is far from complete. In particular, in our own biased opinion, the following items represent the principal areas of deficiency, in decreasing order of importance:

- theoretical understanding of the finite-size scaling behavior at criticality;
- rigorous results concerning the validity of the algorithm;
- the extension of the algorithm to systems other than the q-state Potts ferromagnets.

The first two matters have been discussed in [8] and represent essentially uncharted territory. The third topic is a concern of cluster algorithms in general and is the principal focus of this work.

Based on a notable insight concerning the original Swendsen–Wang (SW) algorithm, Edwards and Sokal [4] proposed a generalization of this algorithm to "arbitrary" spin-systems. However, when applied to particular problems, e.g. the 2-d XY model, the algorithm met with limited success. The key pitfalls of this and other similar approaches were pointed out in [1]. The problems fall into two (related) categories: Strong interactions between separate clusters and the generation of clusters that are impractically large. The first difficulty was neatly circumvented by a decoupling technique that defines a broad class of cluster algorithms. However, the second problem is often in force for any particular algorithm. Indeed, it seems that this problem can only be avoided when the active elements of the graphical representation form large-scale clusters just at the transition point of the spin-system.

The class of algorithms considered in [1] is indeed quite general: for a given spin configuration, a definition is provided for the formation of random clusters, that satisfy an energy constraint. These clusters operate independently of each other and the rest of the system; transitions within the cluster that satisfy the constraint are permitted

which generates the new spin configuration. Unfortunately, the procedure is rather non-specific, in particular with regard to the sanctioned transitions within a cluster. Needless to say, almost any cluster method is a special case of the rules spelled out in [1]. Most of what we derive in this work will fall into this class, if not that of [4].

Our approach is considerably *less* general with regard to the systems discussed and is targeted at *more* specific phenomena. We start with a graphical representation for a certain class of discrete spin-systems that is a straightforward generalization of the FK representation for the Potts model. We show that these systems admit SW (and therefore IC) algorithms. The graphical representations are of interest in their own right; in particular they provide non-pertubative criteria for high-temperature behavior. However, they may be ill-suited for simulations in systems with a continuous transition directly into the low-temperature phase: First off, the SW versions satisfy a Li–Sokal bound but more importantly, even the IC versions will usually suffer from the "big cluster problem" discussed in [1]. Notwithstanding, the two provisos in the previous sentence are often violated: spin systems can have intermediate phases and phase transitions are (generically) discontinuous. The bulk of this paper is concerned with examples where these phenomena can be characterized by a percolation transition in the graphical representation. Along the way, modifications of the representation are developed (for special cases) that circumvent the slowing caused by the presence of an unwanted large cluster at the threshold of low-temperature behavior.

In a future paper, we will describe a similar set of ideas as applied to lattice gasses, along with their continuum limits, random surface models and various other correlated graphical systems. This paper is organized as follows:

(1) In Section 2, we develop a general representation for q-state ferromagnets that can be used for the construction of SW algorithms. With the help of some comparison inequalities, these representations are used to derive necessary conditions for the onset of long-range order. Finally, we discuss the circumstances under which these representations may be useful for the direct simulation of phase transitions; in particular for first-order transitions and for intermediate phases. In Appendix A, we show that the SW algorithms associated with these graphical representations satisfy an inequality of the Li–Sokal type.

(2) In Section 3, we study in detail the Ashkin–Teller (AT) model. For one region of parameters (where there is an intermediate phase) we prove that the representation developed in Section 2 provides a sharp criterion for the onset of long-range order. A refinement of this representation exhibits the onset of low-temperature behavior as a secondary percolation phenomenon. Thus, all known phases in this region are characterized by the geometric phase transitions of this (extended) representation. In the other portion of parameter space, we develop a different representation for the model that seems to have captured all the essential features in this region. For both regions, the graphical representation is easily generalized from the 4 ($= 2 \times 2$)-state AT model to the $q(=r \times s)$-state cubic (or "N_α, N_β") models introduced in [9,10]. However, the representation extends to non-integer values of q. General features of the phase diagram are proved by means of the graphical representation. In Appendix B, we use

the representation to derive duality relations for these spin systems in $d=2$. Although some of these are well known e.g. [11,10] here they apply to the non-integer cases. Under some additional restrictions, the duality in the graphical representation allows a proof that certain transitions actually take place on the self-dual curves.

(3) In Section 4 we show that these representations are easily and efficiently welded together with the techniques of reflection positivity. This combination is then used to prove discontinuous transitions in a variety of "large entropy" models including models with intermediate phases characterized only by short-ranged order.

2. q-state ferromagnets

2.1. A generalized random cluster representation

The graphical representations presented in this section, as well as their derivation, are a straightforward generalization of the FK representation for the Potts models. We will treat ferromagnets with q equivalent internal states. To help get started, let us initially dispense with all superfluous generalities and agree to add the amenities later. We therefore consider a lattice Λ that is a finite piece of the d-dimensional hypercubic lattice $\mathbb{Z}^d$. To each site $i \in \Lambda$, there is a spin variable that can take on one of q values: $\sigma_i \in \{1,2,\ldots,q\}$. If two sites in Λ, i and j, are nearest neighbors and have spin values σ_i and σ_j, the *energy* is given by some function $\mathscr{E}(\sigma_i,\sigma_j)$. We will temporarily assume that there are no other interactions and that the energy function respects the additive group structure: $\mathscr{E}(\sigma_i,\sigma_j)=\mathscr{E}(\sigma_i+\alpha,\sigma_j+\alpha)$, $\alpha=1,2,\ldots$ where addition is understood to be modulo q. On physical grounds, we must have $\mathscr{E}(\sigma_i,\sigma_j)=\mathscr{E}(\sigma_j,\sigma_i)$ and to justify the use of the word ferromagnetic, we will assume that for all α,

$$\mathscr{E}(1,\alpha)\geqslant\mathscr{E}(1,1)\,. \tag{2.1}$$

The Hamiltonian is given by

$$\mathscr{H}=\sum_{\langle i,j\rangle}\mathscr{E}(\sigma_i,\sigma_j) \tag{2.2}$$

where $\langle i,j\rangle$ is here considered to be a *directed* bond from i to j. (In particular, the lattice is oriented for once and all and each bond appears only once in the sum.) For a given bond, we may write

$$\mathscr{E}(\sigma_i,\sigma_j)=\mathscr{E}(1,1)\chi_{\sigma_j=\sigma_i}+\mathscr{E}(1,2)\chi_{\sigma_j=\sigma_i+1}+\cdots+\mathscr{E}(1,q)\chi_{\sigma_j=\sigma_i+q-1} \tag{2.3}$$

where $\chi_{a=b}$ is one if $a=b$ and zero otherwise. Since the energies in Eq. (2.3) are not, in general, in increasing order, let us rewrite this equation:

$$\mathscr{E}(\sigma_i,\sigma_j)=\mathscr{E}_0\chi_{\sigma_j=\sigma_i}+\mathscr{E}_1\chi_{\sigma_j=\sigma_i+\alpha_1}+\cdots+\mathscr{E}_{q-1}\chi_{\sigma_j=\sigma_i+\alpha_{q-1}} \tag{2.4}$$

where $\mathscr{E}_j=\mathscr{E}(1,1+\alpha_j)$ and it is assumed that $\mathscr{E}_0\leqslant\mathscr{E}_1\leqslant\cdots\leqslant\mathscr{E}_{q-1}$. Finally, let us assume, without loss of generality, that the highest energy is zero. Thus, in Eq. (2.4),

there are no more than $q-1$ non-zero terms corresponding to the energies $\mathscr{E}_0,\ldots,\mathscr{E}_k$ with $k+1\leqslant q-1$.

The partition function $Z_{\Lambda,\beta}$ at inverse temperature β is defined by $\mathrm{TR}[e^{-\beta\mathscr{H}}]$ where $\mathrm{TR}[-]$ means sum over all spin configurations with a priori equal weights.[2] Notice that in accord with the fine print of the above definitions, what we have actually defined is the partition function with free boundary conditions. This will simplify the forthcoming derivation; the necessary modifications will be attended to later. The partition function now admits the expression

$$Z_\Lambda = \mathrm{TR}\prod_{\langle i,j\rangle\in\Lambda} e^{-\beta[\mathscr{E}_0\chi_{\sigma_j=\sigma_i}+\cdots+\mathscr{E}_k\chi_{\sigma_j=\sigma_i+\alpha_k}]}. \tag{2.5}$$

The above may be expanded in the standard fashion:

$$Z_\Lambda = \mathrm{TR}\prod_{\langle i,j\rangle\in\Lambda}[1+R_0\chi_{\sigma_j=\sigma_i}][\ldots][1+R_k\chi_{\sigma_j=\sigma_i+\alpha_k}] \tag{2.6}$$

with $R_j = e^{\beta|\mathscr{E}_{\alpha_j}|}-1$. Opening up the product into individual factors, we may imagine k different types of bonds, colors, with a bond occupied in the rth color if the factor $R_r\chi_{\sigma_j=\sigma_i+\alpha_r}$ is selected. If no color is selected, the bond will be called vacant. Notice that (at least once the trace is performed) no two colors can be on the same bond because the product of the χ's is automatically zero and such terms may be omitted in the expansion. The lattice is now divided into multicolored connected clusters. Observe, however, that there will be additional constraints: Suppose that some of the occupied bonds form a loop. Moving around the loop, each color tells the successive spin to move up or down by the amount α_r, the sign of the change depending on the fixed orientation of the bond relative to the direction that it is being traversed. Obviously, the oriented sum of these α_r's must equal zero mod q. It is clear that if this holds for all occupied loops the bond configuration is "consistent" with an actual spin configuration and vice versa.

Let $\bar{\omega}$ denote a generic multicolored bond configuration and let $\mathbf{D}(\bar{\omega})$ be one if all the connected clusters of $\bar{\omega}$ are consistent as discussed above and zero otherwise. For each $\bar{\omega}$ such that $\mathbf{D}(\bar{\omega})=1$ the weight is

$$W(\bar{\omega}) = \prod_{t=1}^{k} R_t^{N_t(\bar{\omega})}\,\mathrm{TR}\prod_{\langle i,j\rangle\in\bar{\omega}}\chi_{\sigma_j=\sigma_i+\alpha_{\langle i,j\rangle}} \tag{2.7}$$

where $N_t(\bar{\omega})$ is the number of bonds of type t in the configuration $\bar{\omega}$ and $\alpha_{\langle i,j\rangle}(\bar{\omega})$ denotes the color of the bond $\langle i,j\rangle$ in $\bar{\omega}$.

It is not difficult to see that the result of the trace is exactly the same as in the case of the standard random cluster models: Given the value of any particular spin in a cluster, the value of every other spin is completely determined. Since the "particular

[2] Here we are primarily interested in problems with *equivalent* spin states. Asymmetries can, in principle, be incorporated by means of "ghost sites". However, except for the simplest cases, these modifications turn out to be somewhat intricate and we will refrain from a discussion of these problems.

spin" can be in any one of q states (recall that for simplicity, we have assumed free boundary conditions on Λ) we get q raised to the number of connected components of the configuration. Thus, we have a generalization of the random cluster measures with weights of multicolored bond configurations given by

$$W(\bar{\omega}) = \mathbf{D}(\bar{\omega}) \prod_{t=0}^{k} R_t^{N_t(\bar{\omega})} q^{c(\bar{\omega})} \tag{2.8}$$

where $c(\bar{\omega})$ is the number of connected components, including isolated sites, of the configuration $\bar{\omega}$. These weights, here expressed in their least refined form, serve as the basis of a well-posed graphical problem. We will develop the representation further but first, a few comments are in order.

2.1.1. Remarks and generalizations

(i) In the case of the Potts models, it is seen that the above reduces to the usual weights of the FK representation; here there is only one color and R_0 is related to the usual parameter p by $R_0 = p/(1-p)$. (To obtain the commonly used formula, multiply the weight of each graph by $(1-p)$ raised to the power of the total number of bonds in Λ.) This parameterization gives the problem a percolation-like character. A similar parameterization is available here as well but is more appropriate for the Swendsen–Wang algorithms that will be presented in the next subsection.

(ii) With a few obvious modifications, a similar representation can be derived for arbitrary boundary conditions. As in the case of the Potts models, these differences are mostly reflected in the counting of $c(\bar{\omega})$. For example, if we wish to consider a fixed spin configuration on the boundary of Λ, we need to place the appropriate colored bonds between the neighboring sites on the boundary and now count all clusters that are connected to the boundary as a single component. It should be observed that these additional "permanent" boundary bonds introduce additional constraints that have to be satisfied by the configuration as a whole.

(iii) The generalization to longer-ranged interactions is straightforward: For pair interactions, we allow for the possibility of (directed) bonds, with appropriate weights, connecting the sites that are supposed to be interacting. For multispin interactions, one can use other geometric objects, triangles, plaquettes, etc., weighted appropriately, all of which are best thought of as constraining directed graphs that connect the interacting sites. Similarly, this sort of representation can be defined for these models on any lattice.

(iv) We have assumed, for simplicity, that the systems under consideration have an additive group structure describing the q-fold equivalence. Clearly this need not be the case and it does not cover problems that are conceivably of interest. For example, suppose that each $\vec{\sigma}_i$ lies on the corners of a rectangle: $\vec{\sigma}_i = (\pm 1, \pm b)$ and that $\mathscr{E}(\vec{\sigma}_i, \vec{\sigma}_j) = -\vec{\sigma}_i \cdot \vec{\sigma}_j + \text{const}$. If $b = 1$, this is just the four state clock model but for $b \neq 1$ this is an asymmetric Ashkin–Teller model. Such a system does not satisfy "$\mathscr{E}(\sigma_i + \alpha, \sigma_j + \alpha) = \mathscr{E}(\sigma_i, \sigma_j)$" and yet can obviously be treated by these methods. The

desired internal symmetry condition can be formulated as follows: Let $T_2, \dots T_q$ denote different permutations of $\{1, \dots, q\}$ (we will take T_1 to be the identity) satisfying $T_k(1) = k$, $k = 1, \dots, q$ and, in general, for any α, $\{T_1(\alpha), \dots, T_q(\alpha)\} = \{1, \dots q\}$. Then, for some such set of T's, the energy is required to satisfy $\mathscr{E}(\sigma_i, \sigma_j) = \mathscr{E}(T_k(\sigma_i), T_k(\sigma_j))$ for each k and for all values of (σ_i, σ_j). (In the above-mentioned example, we may take T_2, T_3 and T_4 as the reflections along the midlines and the product thereof.) For systems that satisfy these more general conditions, it is not awfully difficult to see that a derivation along the preceding lines follows pretty much the same course.

(v) These representations are *faithful* representations of the corresponding spin systems meaning that, in finite volume with fixed boundary conditions, the Gibbs distribution is completely determined by the distributional properties of the graphical representation. Indeed, we have noted that the assignment of a value to a single spin in a cluster completely determines the value of all other spins in the cluster. If a cluster is connected to the boundary (corresponding to a fixed value of the boundary spins) then we know the spin values inside the cluster and if the cluster is detached, there are q equally likely possibilities. Thus, following the proof in [12] (Section 2.1) for the usual FK representation, the expectation of any observable in the spin system can be computed by knowing the statistics, including the colors, of the clusters in the graphical representation.

The generalizations discussed above will be implicitly assumed in the remainder of this section unless explicitly stated otherwise. However, the notation will continue along the user-friendly lines and the missing provisos and extra details will be left to the reader.

As things stand, the above representations are more or less on a par with standard high- or low-temperature representations – although here these enjoy the slight distinction of being both simultaneously. Furthermore, percolation and long-ranged order are related in this representation: As will be demonstrated in Proposition 2.2, the absence of percolation in this representation indicates high-temperature behavior in the spin system. (This will be made precise in the statement of the proposition.) In several cases, the converse is true as will be demonstrated in Sections 3 and 4. We will pursue these lines of discussion after some further development of the high-temperature properties of this representation.

The distinguishing feature of the FK random cluster representation is that the representation itself enjoys the FKG property. (We will assume that the reader is familiar with these matters. A complete treatment can be found, for example, in [13].) However, it is unlikely that in the present form, this could ever be proved for the more general representations: Any reasonable attempt at a partial ordering of the bonds will inevitably lead to violations of the consistency condition as we "raise" the configuration. We can avoid facing such difficulties head on by considering the measure that focuses only on the bonds that are occupied and weighting each configuration in accord with all legitimate coloring schemes. In certain cases, we can show that this leads to measures with the FKG property and in general, it permits comparison inequalities between these and random cluster measures with appropriate values of parameters.

Lemma 2.1. Let $\mathscr{H}$ denote the Hamiltonian of a q–state ferromagnet of the type described with non-zero energies $\mathscr{E}_0, \ldots \mathscr{E}_k$ let β denote an inverse temperature and let Λ denote a finite lattice. Consider the measures $\mu^*_{\mathscr{H};\beta}(-)$ that assign the probability to the uncolored (grey) bond configuration ω given by the sum of the probabilities in the measure defined by the weights in Eq. (2.8) of all the allowed colorings of this configuration, with $*$ denoting various appropriate boundary conditions for the graphical problem (e.g. free). Let β be the inverse temperature defined by

$$e^{\bar{\beta}} - 1 = R_0 + \cdots + R_k$$

and let $\mu^{FK;*}_{q,p}(-)$ denote the random cluster measures with parameters q and $p \geqslant 1 - e^{-\bar{\beta}}$. Then, for boundary conditions in which $\mu^{FK;*}_{q,p}(-)$ is itself FKG, including free and wired,

$$\mu^{FK;*}_{q,p}(-) \underset{\text{FKG}}{\geqslant} \mu^*_{\mathscr{H};\beta}(-) .$$

Proof. Let us start with a construction of the measures $\mu^*_{\mathscr{H};\beta}(-)$ with $* = f$ corresponding to free boundary conditions on Λ. Let ω denote a bond configuration on Λ and let $\mathfrak{s}(\omega)$ denote a coloring *scheme* (in which one of the $(k+1)$ colors are assigned to each bond of ω). Let $R = R_0 + \cdots + R_k$ and let r_j be defined by

$$r_j = R_j / R . \tag{2.9}$$

Notice that $\sum_j r_j = 1$. Obviously, the collection $(\omega; \mathfrak{s}(\omega))$ is in one-to-one correspondence with the preceding multicolored $\bar{\omega}$'s. We may write

$$\mu^f_{\mathscr{H};\beta}(\omega) \propto q^{c(\omega)} R^{N(\omega)} \sum_{\mathfrak{s}(\omega)} B_{\mathbf{r}}(\mathfrak{s}(\omega)) \mathbf{D}(\mathfrak{s}(\omega)) . \tag{2.10}$$

In the above, $N(\omega)$ and $c(\omega)$ are, respectively, the number of bonds and the number of connected components of the uncolored ω, $B_{\mathbf{r}}(\mathfrak{s}(\omega))$ is the Bernoulli probability of the coloring scheme $\mathfrak{s}(\omega)$ using $\mathbf{r} = r_0, \ldots, r_k$ for the probabilities of the possible colors and, finally, $\mathbf{D}(-)$ has the same meaning as before.

Other boundary conditions that are of interest have additional sites in the complement of Λ that may be connected to sites in Λ by additional bonds. Certain of these additional sites are connected to one another via their own fixed colored bonds (or weighted combinations thereof) that in and of themselves are a consistent scheme. Under these circumstances, $\mu^*_{\mathscr{H};\beta}(-)$ is determined by a formula identical to Eq. (2.10) with the appropriate modification of the counting of the number of connected components and the insistence that $\mathfrak{s}(\omega)$ satisfy the additional constraints. To keep our notation at a manageable level, we will usually forfeit the privilege of adding a $*$ to the quantities c and $\mathbf{D}$ and allow these modifications to be inferred from context.

Now the right-hand side of Eq. (2.10) looks like (the numerator of) the expectation of a function, namely $\sum_{\mathfrak{s}(\omega)} B(\mathfrak{s}(\omega)) \mathbf{D}(\mathfrak{s}(\omega))$, with respect to the random cluster measure at parameters q and λ with $\lambda/(1-\lambda) = R$. Provided that this random cluster measure is itself FKG, it is sufficient to show that the above-mentioned function is

decreasing. For free boundary conditions or for the more general boundary conditions (obtained by the stipulation that some boundary sites are connected to others in the complement of Λ) the random cluster measures are indeed FKG for all $q \geqslant 1$. Thus, let us turn to the task of showing that the additional factor constitutes a decreasing function.

To this end, let $\omega \subset \omega'$. Writing $\omega' = \omega \cup \eta$ with $\omega \cap \eta = \emptyset$, let $\mathfrak{s}(\omega)$ and $\tilde{\mathfrak{s}}(\eta)$ denote colorings of ω and η. Further, let us use $(\mathfrak{s}(\omega), \tilde{\mathfrak{s}}(\eta))$ as notation for the combined coloring as applied to the configuration ω'. We may write $\mathbf{D}(\mathfrak{s}(\omega), \tilde{\mathfrak{s}}(\eta)) = \mathbf{D}(\mathfrak{s}(\omega)) \cdot \mathbf{D}(\tilde{\mathfrak{s}}(\eta) \mid \mathfrak{s}(\omega))$ where the first factor indicates if $\mathfrak{s}(\omega)$ is a respectable coloring of ω and the second $\mathbf{D}$-factor is non-zero only if $\tilde{\mathfrak{s}}(\eta)$ is a "good coloring" of the rest of ω' *given* the coloring $\mathfrak{s}(\omega)$. Thus we have

$$\sum_{\mathfrak{s}''(\omega')} B(\mathfrak{s}''(\omega'))\mathbf{D}(\mathfrak{s}''(\omega')) = \sum_{\mathfrak{s}(\omega), \tilde{\mathfrak{s}}(\eta)} B(\mathfrak{s}(\omega))B(\tilde{\mathfrak{s}}(\eta))\mathbf{D}(\mathfrak{s}(\omega))\mathbf{D}(\tilde{\mathfrak{s}}(\eta) \mid \mathfrak{s}(\omega)) . \tag{2.11}$$

But the term $\mathbf{D}(\tilde{\mathfrak{s}}(\eta) \mid \mathfrak{s}(\omega))$ never exceeds one; setting it to one, the unrestricted sum over $\tilde{\mathfrak{s}}(\eta)$ is exactly one and this amounts to a statement of the desired monotonicity. □

These domination inequalities are useful in conjunction with the following definition and elementary result:

Definition. Consider a generalized random cluster model of the type described above, in a finite lattice Λ with $*$ for a boundary condition. Let $P^*_{\Lambda,i}(\beta)$ denote the probability that the site i is connected to the boundary and let

$$P_{\Lambda,i}(\beta) = \max_{*} P^*_{\Lambda,i}(\beta)$$

denote this probability given the optimal boundary condition on Λ. We will say that there is no percolation if for every (fixed) i, and for every increasing sequence of lattices that exhaust all of $\mathbb{Z}^d$,

$$\lim_{\Lambda \nearrow \mathbb{Z}^d} P_{\Lambda,i}(\beta) = 0 .$$

Proposition 2.2. Suppose, for a spin model of the type described, that at inverse temperature β, there is no percolation in the graphical representation. Then there is no symmetry breaking in the sense that if $\langle - \rangle_{\mathscr{H};\beta}$ is any infinite volume Gibbs state of the Hamiltonian $\mathscr{H}$ at inverse temperature β, F is any summable function of spin configurations $(\underline{\sigma})$, and $F^{[\alpha]}$ is the function defined (pointwise a.e.) by

$$F^{[\alpha]}(\underline{\sigma}) = F(\underline{\sigma} + \underline{\alpha})$$

where $(\underline{\sigma} + \underline{\alpha})$ is the configuration obtained from $(\underline{\sigma})$ by adding α to the value of $(\underline{\sigma})$ at each site then $\langle F^{[\alpha]} \rangle_{\mathscr{H};\beta} = \langle F \rangle_{\mathscr{H};\beta}$. In particular, the spontaneous magnetization

vanishes. Furthermore, there is high-temperature decay of correlations in the sense that if $G(\alpha_1,\dots,\alpha_n)$ is any function of n spin variables with

$$0=\sum_{\alpha_1,\dots,\alpha_n} G(\alpha_1,\dots,\alpha_n)$$

then $\langle G(\sigma_{i_1},\dots,\sigma_{i_n})\rangle_{\mathscr{H};\beta} \to 0$ as the minimum separation between any of the points tends to infinity. In particular, the n-point correlation functions tend to zero as the points become well separated.

Proof. Focusing first on the magnetization, the contribution from the ith site to the magnetization vanishes in those graphical configurations in which i is detached from the boundary. Thus, without percolation there is no magnetization. In more generality, it is sufficient to consider F's that depend on only finitely many coordinates. Let $F=F(\sigma_{i_1},\dots,\sigma_{i_k})$ denote one such function and let $\langle - \rangle^{\Lambda;\#}_{\mathscr{H};\beta}$ denote the Gibbs distribution for the spin system in finite volume Λ with boundary condition #. Let $\mathscr{J}_\alpha(\#)$ denote the boundary conditions identical to # except that each spin on the boundary has been "jacked" down by the amount α. It is clear, by relabeling, that

$$\langle F^{[\alpha]}\rangle^{\Lambda;\#}_{\mathscr{H};\beta} \equiv \langle F(\sigma_{i_1}+\alpha,\dots,\sigma_{i_k}+\alpha)\rangle^{\Lambda;\#}_{\mathscr{H};\beta} = \langle F\rangle^{\Lambda;\mathscr{J}_\alpha(\#)}_{\mathscr{H};\beta}. \tag{2.12}$$

However, the graphical representations corresponding to # and $\mathscr{J}_\alpha(\#)$ are identical and thus the contributions to $\langle F\rangle^{\Lambda;\#}_{\mathscr{H};\beta}$ and $\langle F\rangle^{\Lambda;\mathscr{J}_\alpha(\#)}_{\mathscr{H};\beta}$ are identical from all configurations $\bar{\omega}$ in which the sites $i_1,\dots,i_k$ are detached from the boundary. Hence, we may estimate:

$$|\langle F-F^{[\alpha]}\rangle^{\Lambda;\#}_{\mathscr{H};\beta}| \leqslant |F_{\max}-F_{\min}|[P_{\Lambda,i_1}(\beta)+\cdots+P_{\Lambda,i_k}(\beta)] \to 0 \tag{2.13}$$

as $\Lambda \nearrow \mathbb{Z}^d$, which implies that in any limiting state, the average of F and $F^{[\alpha]}$ are equal.

Similarly, if $G(\sigma_{i_1},\dots,\sigma_{i_n})$ is a function as described in the statement of this proposition, it is clear that the contributions to $\langle G\rangle^{\Lambda;\#}_{\mathscr{H};\beta}$ from configurations $\bar{\omega}$ vanish unless some pair of sites from $i_1,\dots,i_n$ are connected in $\bar{\omega}$. (Including, of course, the possibility of a connection via the component of the boundary sites.) However, this has negligible probability for large separation: Suppose that i and j are sites with maximum difference in coordinates equal to l. Let $\Lambda_l(i)$ denote a hypercube of side l centered at i (so that j is on the boundary of i). If $\Lambda \supset \Lambda_l(i)$, the probability that i is connected to j, with any boundary conditions on Λ, is surely less than the probability that i is connected to the boundary of $\Lambda_l(i)$ with boundary conditions on $\Lambda_l(i)$ chosen so as to optimize this probability, i.e. $P_{\Lambda_l(i),i}(\beta)$. Thus, for minimum separation between the sites $i_1,\dots,i_n$ large, as $\Lambda \nearrow \mathbb{Z}^d$, the average $\langle G\rangle^{\Lambda;\#}_{\mathscr{H};\beta}$ cannot exceed some small number that vanishes with increasing separation. This implies the desired result. □

As a consequence of the above we have:

Corollary. Let $p_c(q)$ denote the parameter value in the random cluster model at which percolation first sets in. Let $\pi_c(q)\leqslant p_c(q)$ denote the largest value of p

below which there is always exponential decay of correlations. Then, for the general q-state ferromagnets discussed in the above propositions, if $R < p_c(q)/(1 - p_c(q))$, there is no symmetry breaking and there is high-temperature clustering of correlations. If $R < \pi_c(q)/(1 - \pi_c(q))$, the clustering is exponential.

Remark. It is widely accepted that in general, $p_c(q) = \pi_c(q)$. For $q = 2$, this was established on the square lattice by exact solution [14] and, in quite some generality in [15]. For $q \gg 1$, this follows implicitly from any of the classic large q treatments of the Potts model, e.g. [16,17] or [18]. Explicit details will be presented in Section 4.

Proof. If $p < p_c(q)$, the consequences of no percolation in the FK random cluster models carry over to the generalized random cluster problems by the domination lemma whenever $R < p_c(q)/(1 - p_c(q))$. The conclusions about the absence of symmetry breaking and the clustering of correlations follow from Proposition 2.2. Further, if $R < \pi_c(q)/(1 - \pi_c(q))$, the decay of correlations is exponential. □

Remark. Even assuming the stronger condition, the above does not prove the best possible result: unicity of the limiting Gibbs state (or that of the associated random cluster measure). A complete proof might follow from some further analysis and/or would follow if FKG properties in the generalized random cluster measure could be established. As for the latter, we have several examples where this can be proved but no general results in this direction. In any event, both lines of attack are currently under investigation.

2.2. Swendsen–Wang algorithms

In accord with the primary goals of this paper, we will devote this subsection to a demonstration that the q-state ferromagnets just described admit SW-type algorithms. The principal feature of this subsection will be an explicit verbal description of the algorithm, thus we will restrict our attention to the simplest algorithms for the user friendly cases. In Appendix A, we will discuss these algorithms and the various generalizations from the perspective of Li–Sokal bounds. Apparently, all of the algorithms are special cases of the algorithms described in Section 2 of [1]. However these have the advantage of a closed form expression for the Edwards–Sokal weights so that various properties, e.g. detailed balance, are manifestly apparent.

2.2.1. Description of the algorithm

Let $\Lambda \subset \mathbb{Z}^d$ be a finite lattice with free (or periodic) boundary conditions and consider a nearest neighbor q-state ferromagnet with Hamiltonian as described in Eq. (2.2) (with the additive version of the internal symmetry) on Λ. Let $p_0, p_1, \ldots, p_k$ be defined by

$p_j = R_j/[R_j+1]$ where the R_j's are defined below Eq. (2.6). The algorithm is described as follows:

Step 0: Start with a spin configuration, σ_Λ, on this lattice.

Step 1: On each directed bond $\langle i,j\rangle$ in Λ check whether $\sigma_j = \sigma_i + \alpha_s$ for some $s = 0,\ldots,k$. If this is the case, then with probability p_s place the sth-type bond between σ_j and σ_i and with probability $(1-p_s)$, do nothing. If $\sigma_j \neq \sigma_i + \alpha_s$ for any s (i.e. if the spins are in a zero energy state) then do nothing. This procedure is done independently for each bond of the lattice.

Step 2: The lattice is now divided into connected clusters. Erasing the existing spin configuration, there are exactly q spin configurations in each cluster that are consistent with the bond coloring scheme tying the cluster together. For each cluster, including the isolated sites, independently pick one of these q allowed configurations. This completes step 2; erasing all bonds brings us back to step 0.

The following is readily established:

Proposition 2.3. The above described algorithms satisfy detailed balance: For the spins, this is with respect to the Gibbs state corresponding to the appropriate Hamiltonian as written in Eq. (2.2). For the bonds, this is with respect to the appropriate random cluster measures as in Eq. (2.8) or Eq. (2.10).

Proof (*Kandel and Domany* [1] *and Edwards and Sokal* [4]). It is noted that the algorithm simulates the joint measure on bond-spin configurations $(\bar{\omega}_\Lambda, \sigma_\Lambda)$ that has the weights

$$W(\bar{\omega}_\Lambda, \sigma_\Lambda) = \Delta(\bar{\omega}_\Lambda, \sigma_\Lambda) \prod_{j=0}^{k} B_{p_j}(\bar{\omega}_\Lambda) \tag{2.14}$$

where $\Delta(\bar{\omega}_\Lambda, \sigma_\Lambda)$ is one if the bond-spin configuration is "consistent" and zero otherwise and where

$$B_{p_j}(\bar{\omega}_\Lambda) = p_j^{N_j(\bar{\omega}_\Lambda)}(1-p_j)^{\mathbb{B}_\Lambda - N_j(\bar{\omega}_\Lambda)} \tag{2.15}$$

is the Bernoulli factor for the configuration of bonds of the jth color with $\mathbb{B}_\Lambda$ denoting the total number of bonds in Λ. Each move of the algorithm is now interpreted as "applying the conditional distributions" and it is not hard to verify that the marginals of (2.15) are exactly the appropriate Gibbs distribution for the spins and the random cluster measures for the bonds. □

We now turn attention to the most pertinent facet of this subsection: When might we expect these algorithms to be useful?

As was demonstrated in the previous subsection, percolation in the graphical representation is required for low-temperature behavior. Unfortunately, for ferromagnets, this sort of percolation is not sufficient. For the purposes of the present discussion, let us assume that $\mathscr{E}(\alpha,\alpha) < \mathscr{E}(\alpha,\alpha')$ for $\alpha \neq \alpha'$ (so that for $d \geqslant 2$, there is always a low-temperature magnetized phase). Furthermore, here and throughout the remainder

of this paper, we will refer to the low energy bonds in the multicolored representation as "blue" and to the (generic) bonds of the measures defined in Eq. (2.10) as "grey".

It would seem that some form of percolation of the *blue* bonds is required in order to have magnetic ordering in the spin system. (Notwithstanding, this appears to be difficult to prove in the general case. For the additive version of the 4-state models where the pairing energy increases with the distance of the spin states, a nearly complete statement can be made: blue percolation for *some* boundary conditions is a necessary condition and with a particular boundary condition a sufficient condition for magnetic ordering. Since this result is rather limited in scope, its proof will be relegated to Section B.3 of Appendix B.) And worse yet, in the general case, mere percolation of the blue bonds is not sufficient – cf. the discussion following the proof of Theorem 3.3 and [19]. However, even in a system where percolation of blue bonds is necessary and sufficient for magnetic ordering, it is easy to envision what will go wrong with this representation: Spontaneous magnetization will not occur until the formation of infinite clusters of blues but multicolored infinite clusters, without infinite subclusters of blues, are bound to form at higher temperatures simply because there are more players on the team. In particular, this "false percolation" obviously occurs if the different colored bonds are independent and, to be definitive, on the Bethe lattice for the four state model described in the above parenthetic remark [20].

Thus, the general implication is that the percolation threshold in the grey representation is at a higher temperature then the transition temperature for magnetic ordering. What is more, in the context of an actual simulation, if the grey infinite cluster occupies a significant fraction of the lattice at the magnetic ordering temperature, we have walked right into the "large cluster problem" discussed in [1]. It is almost certain that we will experience severe slowing down under SW dynamics and doubtless that there will be slowing down under IC dynamics as well. However, regarding these representations on the whole, there are two important possibilities that have been overlooked:

(A) The possibility that the grey percolation transition is signaling the presence of another phase that is different from the low-temperature magnetized phase.

(B) The possibility of a first-order transition in the grey representation where the infinite cluster density is discontinuous at threshold. This almost certainly indicates that there is a first-order transition in the spin system. Under such circumstances, the intuition that was exploited in the preceding paragraph is no longer applicable: The transition could be into an intermediate phase or directly into the low-temperature phase. The former case falls under item (A) and in the latter case, magnetic ordering indeed coincides with the grey percolation transition.

We will explore these two possibilities in the remainder of this paper. In the context of the Ashkin–Teller model we will show (Section 3.2, The Reformed Ferromagnetic Region) that percolation in the grey representation targets perfectly the intermediate phases in these systems. Similar results hold for a generalization of the AT models. In the following section, for a slightly restricted class of models (the nearest-neighbor additive cases on $\mathbb{Z}^d$) we will show how these graphical representations can be used in conjunction with reflection positivity. Using the techniques pioneered in [16] we

will demonstrate that (B) is in fact quite typical for large q models with relatively few low-lying energy states. In many cases, we will show that this leads to a transition directly into the magnetically ordered phase and in any case, for these systems, the discontinuous transitions in the grey representation imply first-order transitions in the spin system.

However, beyond the Potts models, the subject of continuous (or weakly first-order) ferromagnetic transitions out of the high-temperature phase or ferromagnetic transitions out of an intermediate phase remains largely uncharted. As emphasized in the introduction, we believe that at present, the goal of complete generality is over ambitious; problems must be solved on a case-by-case basis. Restricting attention to the user-friendly systems, let us therefore work our way up the list. The cases $q=2$ and $q=3$ are just the Potts models so the first new item is $q=4$, the Ashkin–Teller model. Here there are two distinct lines of ferromagnetic transitions: the first, interpolating between the 4-state clock and Potts transitions is directly out of the high-temperature phase and the second one is out of the intermediate phase. We will prove by overt demonstration that it is possible to treat these transitions by cluster methods. Needless to say, most of the higher spin cases remain both interesting and open.

3. 4-state ferromagnets (and generalized AT models)

3.1. The Ashkin–Teller model

In this section, we will study in detail the case $q=4$. Under the restriction that the interactions enjoy the additive version of the internal symmetry, these are known as the symmetric Ashkin–Teller models [21].[3] We will define graphical representations leading to effective algorithms that exhaust most of the phase diagram in these cases and also discuss the asymmetric cases under certain conditions. Usually, this model is described in terms of a pair of coupled Ising systems. Although we will have to resort to this trick for a portion of our analysis, for the most part, we will treat this as a traditional four state spin system.

Let us start, then, with the symmetric version. We will denote the possible spin states as $0, +1, -1$ and 2 which may be viewed as points on a circle. Under the assumption of additive symmetry, we need only specify a few energies: $\mathscr{E}_{0,0}$, $\mathscr{E}_{0,\pm 1}$ and $\mathscr{E}_{0,2}$. These energies may be displayed in the form of an "energy level diagram" as is done near the bottom of the phase diagram in Fig. 1. Under the constraints of ferromagnetism, there are only two basic possibilities, $\mathscr{E}_{0,2} \geqslant \mathscr{E}_{0,\pm 1}$ or $\mathscr{E}_{0,2} \leqslant \mathscr{E}_{0,\pm 1}$. The boundary case, $\mathscr{E}_{0,2} = \mathscr{E}_{0,\pm 1}$ is, of course, the Potts model. Under the condition $\mathscr{E}_{0,2} \geqslant \mathscr{E}_{0,\pm 1}$, the system is truly ferromagnetic whereas if $\mathscr{E}_{0,2} \leqslant \mathscr{E}_{0,\pm 1}$, the system has a degree of antiferromagnetic character which, as we shall see, opens up some

[3] An interesting historical note: the actual model of interest to Ashkin and Teller was none other than the 4-state Potts model and the general model was defined only to aid in the study of this case. The definitive result of their paper was the location of the self-dual point along this single line in parameter space.

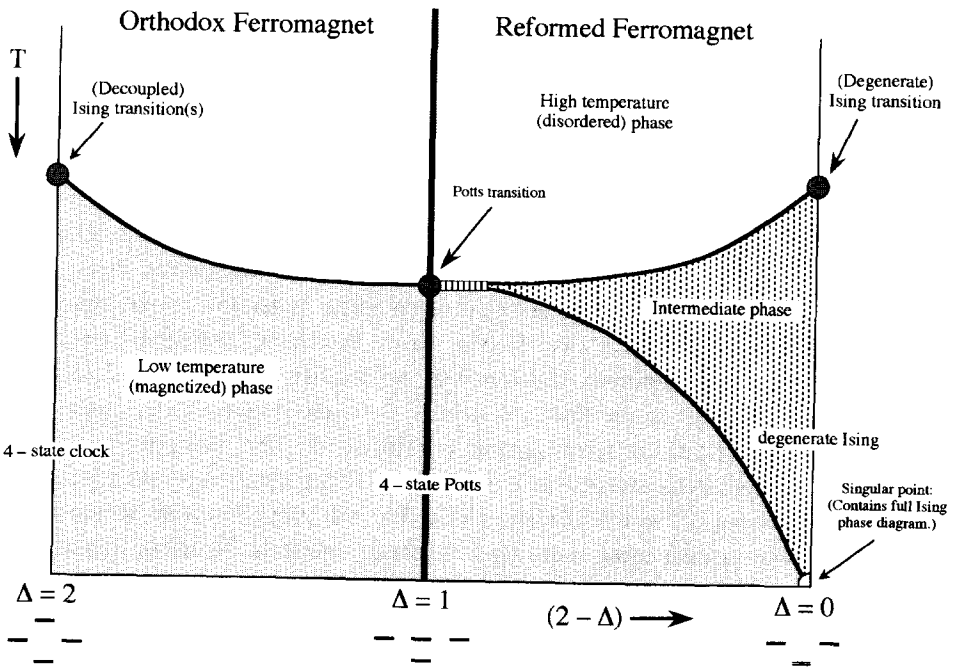

Fig. 1.

interesting possibilities. We will denote these two scenarios as "orthodox ferromagnetic" and "reformed ferromagnetic", respectively.

To keep things at a manageable level, let us fix $\mathscr{E}_{0,\pm 1} - \mathscr{E}_{0,0} \equiv 1$ and define $\Delta \equiv \mathscr{E}_{0,2} - \mathscr{E}_{0,0}$, using temperature and Δ as our variables. The line $\Delta = 2$ corresponds to the usual 4-state clock model which turns out to be equivalent to two decoupled Ising models, the line $\Delta = 1$ is the Potts model and the line $\Delta = 0$ also an Ising magnet. (with a superfluous, decoupled degree of freedom at each site). There are even more Ising magnets hidden inside this model, the subtler ones are *better* seen without the benefit of the Ising-spin representation. For technical reasons, we will not discuss $\Delta > 2$ (except briefly in Section B.3 of Appendix B).

In the phase diagram we will plot T versus $2 - \Delta$. The broad features are as follows: In the orthodox region, there is a single ordering transition into a magnetized state. The phase boundary continues into the reformed region where at some point it splits. (In $d = 2$, this presumably happens at the dividing line between the two regions but in $d > 2$, this probably does *not* happen until $\Delta < 1$.) Between the upper and lower branches of the split line, is a partially ordered phase where the density of one pair of species whose spin values differ by 2 is enhanced. Further details may be read off the figure caption. All of the above, save for the parenthetic remark, will be proved in this section. Much of this was established a while ago in [22].

We will divide this section into two further subsections: The first, constituting the bulk of our analysis, will concern the "reformed ferromagnetic region" $0 \leqslant \Delta \leqslant 1$. Here,

the general representation of the previous section provides us with a canonical example of an intermediate phase on display as a percolation phenomenon. We rewrite the grey measure introduced in Lemma 2.1 replacing the colored degrees of freedom by a related set of variables that we call "black and white". The entire phase structure is characterized by the percolation properties of this representation: The end of high-temperature behavior is signaled by percolation in the grey measure and the onset of the low-temperature phase is indicated by the percolation of black-only degrees of freedom. The intermediate phase occurs precisely when there is the former without the latter. This, without pain, covers and extends the relevant portions of [22]. This representation extends to the natural generalization of the AT models known as the cubic models and for these cases, similar results are established. Finally, we discuss the SW algorithm that is tied to the black and white representation.

In the next subsection, on the "orthodox ferromagnetic region", we will use the Ising-spin representation of this model to derive an entirely different sort of graphical expansion within which the ferromagnetic transition can be understood as a straightforward FK-type percolation problem.

3.2. *The reformed ferromagnetic region*

We turn our attention to the region to the right of the Potts line, $\Delta \leqslant 1$. As will be discussed below, if $|\Delta| < 1$, then $\pm\Delta$ are equivalent. Generally, we will assume that $\Delta > 0$ and discuss things in as ferromagnetic a language as possible.

Let us consider the multicolored representation as defined in Eq. (2.8). Although there are ostensibly three different colors of bonds, raising the spin value by two is the same as lowering it by two, so the corresponding colors are equivalent. This also allows us to do away with the orientation of the lattice; we are down to undirected configurations with two colors. These will be denoted by orange (connecting neighboring pairs that differ by two) and blue (for low-energy pairs). Models of this type that are (more) genuinely antiferromagnetic can be treated within these frameworks: If the lattice is bipartite and $\mathscr{E}_{0,0} > \mathscr{E}_{0,2}$ we can exchange the roles of orange and blue and quietly redo the forthcoming treatment. This is equivalent, in the spin language to the relabeling on one of the sublattices: $(0, \pm 1, 2) \to (2, \mp 1, 0)$. Of course when there are more complicated interactions or more complicated lattices, these simple minded treatments break down. The "antiferromagnetic" models that can be treated yield exactly nothing new and need not be discussed further.

Coming from the high-temperature side, the (first) ordered phase of this model is characterized by an abundance of 0's and 2's over ± 1's – or vice versa. This phase is distinguished from the low-temperature phase because, e.g. in the 0 and 2 – rich phase there are equal amounts of both. In any case, it would seem that percolation point of combined orange and blue clusters – or plain old percolation in the grey representation described in Eq. (2.10) corresponds to the boundary of the high-temperature phase: within each connected cluster, spins either agree or differ by 2. This notion will be made precise after we develop the alternative form of the grey representation.

Definition (*The black and white representation*). Consider the weights of a grey configuration ω as defined in Eq. (2.10); let us denote this object by $W_G^{AT}(\omega)$, temporarily suppressing the dependence on parameters. For simplicity let us discuss only the case of free boundary conditions. First, notice that the sum over all possible colorings of ω factors into the product of (the sum of) all possible colorings of each cluster of ω:

$$W_G^{AT}(\omega) \propto R^{N(\omega)} 4^{c(\omega)} \prod_{j=1}^{k(\omega)} \left[\sum_{\mathfrak{s}(K_j)} B_{(p_b, p_o)}(\mathfrak{s}(K_j)) \mathbf{D}(\mathfrak{s}(K_j)) \right] . \tag{3.1}$$

In the above, $K_j(\omega)$ is the jth connected *bond* cluster of ω – of which there are a total of $k(\omega)$, the object $\mathfrak{s}(K_j)$ denotes a coloring of K_j by orange and blue bonds, $B_{(p_b, p_o)}(\mathfrak{s}(K_j))$ is the Bernoulli factor for this coloring assigning p_b for each blue bond and $p_o = 1 - p_b$ for each orange bond of $\mathfrak{s}$. As usual, the **D** factors tells us which colorings are allowed; here they are written so as to act separately on each cluster.

The key observation is that the cluster coloring factors, the terms in square brackets on the right-hand side of Eq. (3.1), have the interpretation of a partition function for a spin system defined on (the graph of) the cluster. Although this interpretation holds, more or less, for the general cases described in the previous section, here it is the partition function for a ferromagnetic Ising model. Indeed, let K denote any connected cluster. If the value of a single spin in K is fixed, say at 0, then in every legitimate coloring, the value of every other spin in the cluster is uniquely determined: the colorings are in one-to-one correspondence with the possible spin configurations. However, since there are no "red" bonds that allow neighboring spins to differ by one each "spin value" in the cluster (given that one of them was a 0) is either a 0 or a 2. The weight for a given spin configuration/coloring, the Bernoulli term, is a given by factor of p_b for every neighboring pair in agreement and p_o for every pair in the cluster that differs. Identifying $p_b/p_o \equiv e^{\beta_{eff}}$ and summing over all such configurations completes the identification: the 0's are the $+$'s and the 2's are the $-$'s. Let us write the Hamiltonian in Potts form, $\mathscr{H} = -\sum_{\langle ij \rangle \in K_j} [\delta_{\sigma_i, \sigma_j} - 1]$. (Here, of course, the summation takes place only on the edges of the *graph* defined by the cluster K_j.) Then, the precise relationship is

$$\sum_{\mathfrak{s}(K_j)} B_{p_b, p_o}(\mathfrak{s}(K_j)) \mathbf{D}(\mathfrak{s}(K_j)) = \frac{1}{2} p_b^{N(K_j)} Z_f(K_j; \beta_{eff}) \tag{3.2}$$

where $Z_f(-)$ is the Ising partition function with free boundary conditions, $N(K_j)$ is the number of bonds in the cluster K_j and the factor of $\frac{1}{2}$ accounts for the fact that, in contrast to the preceding discussion, we will *not* lock down the value of any particular spin in the cluster. The product of all these terms must be multiplied by $R^{N(\omega)} 4^{c(\omega)}$. We see that $\prod_{j=1}^{k(\omega)} p_b^{N(K_j)} = p_b^{N(\omega)}$ so this will simply redefine the parameter R: $\tilde{R} \equiv p_b R$. Next, let us write $4^{c(\omega)} = 2^{c(\omega)} \times 2^{c(\omega)}$, leave the first factor alone and for the second write $c(\omega) = k(\omega) + I(\omega)$ where $I(\omega)$ is the number of sites left isolated by

the configuration ω. We thus cancel the $(\frac{1}{2})^{k(\omega)}$ and we are left with a factor of 2, the Ising partition function, for each isolated site. We can thus express the weights as an "outside factor", $\tilde{R}^{N(\omega)}2^{c(\omega)}$, times the product of the Ising partition function on each *component* of ω:

$$W_G^{AT}(\omega) = \tilde{R}^{N(\omega)}2^{c(\omega)} \prod_{j=1}^{c(\omega)} Z_f(C_j; \beta_{\text{eff}}) \tag{3.3}$$

where C_j is the jth component of ω. It should not go unnoticed that the outside factors are themselves none other than the random cluster weights for the Ising system.

The next step is to take the Ising partition functions and develop them in a random cluster expansion:

$$Z_f(C_j; \beta_{\text{eff}}) = \sum_{\eta_j \subset C_j} B_a(\eta_j)2^{c(\eta_j)} \tag{3.4}$$

where $B_a(\eta_j)$ is the Bernoulli factor for the configuration η; explicitly, $B_a(\eta_j) = a^{N(\eta_j)}(1-a)^{N(C_j \setminus \eta_j)}$ and in various places, C_j is understood to mean the bonds in C_j and in others, the graph (bonds and sites) itself. Of course here, $a = 1 - e^{-\beta_{\text{eff}}}$. It should be observed that $c(\eta_j)$ is relative to the background of C_j: $c(\eta_j) + N(\eta_j) =$ [# of loops of η_j] + [# of sites in C_j]. If we consider a giant $\eta = \bigcup_j \eta_j$, one η_j for each C_j, the counting works perfectly because the sum of all the sites in all of the C_j's is the total number of sites in the lattice. Thus

$$\sum_j c(\eta_j) = c(\eta) \tag{3.5}$$

where the right-hand side is the number of components relative to the full lattice. We arrive at the formula for the weight of configurations (ω, η) with $\eta \subset \omega$:

$$W_{BW}^{AT}(\omega, \eta) \equiv W_{BW;(g,a)}^{AT}(\omega, \eta) = B_g(\omega)2^{c(\omega)}B_a(\eta)2^{c(\eta)}\chi_{\eta \subset \omega}\,. \tag{3.6a}$$

where $\chi_{\eta \subset \omega}$ enforces the constraint $\eta \subset \omega$.

This is the black and white representation; black bonds are those in η, white bonds are the ones in $\omega \setminus \eta$. It is not hard to show that the derivation and formulas hold for more general boundary conditions. In particular, a generous class of boundary conditions coming from the spin system can be obtained by declaring certain sets of boundary sites to be "preconnected" by white bonds and others by black bonds. In these cases, one need only modify the definition of $c(\omega)$ and $c(\eta)$ as appropriate. Of particular importance will be the *black-wired* boundary conditions meaning that all boundary sites are to be considered as part of the same black component; in the spin system, this corresponds to setting all the boundary spins to the same state.

The form of the weights as written in Eq. (3.6a) is already perfect for the design of cluster algorithms. For the purpose of some of the up and coming analysis, it is better to separate the η and ω terms completely (in Eq. (3.6a), the Bernoulli factor for

η depends on the number of bonds in ω). Thus, writing $B_a(\eta) = a^{N(\eta)}(1-a)^{N(\omega)-N(\eta)}$ and $B_g(\omega) = g^{N(\omega)}(1-g)^{N(\Lambda)-N(\omega)}$, we may say

$$W_{BW}^{AT}(\omega,\eta) \propto U^{N(\omega)}2^{c(\omega)}V^{N(\eta)}2^{c(\eta)}\chi_{\eta\subset\omega} \tag{3.6b}$$

with $V = a/(1-a)$ and $U = g(1-a)/(1-g)$.

The utility of this representation is underscored by the following:

Proposition 3.1. In any finite Λ, the black and white graphical measures as defined by Eq. (3.6), and their extension to various other boundary conditions are a faithful representation of the corresponding AT system at parameters β and Δ with $0 \leqslant \Delta < 1$ and $\beta < \infty$ related to g and a by

$$g = 1 - e^{-\beta}$$

and

$$a = [1 - e^{-\beta\Delta}]/[1 - e^{-\beta}] .$$

or

$$U = e^{\beta(1-\Delta)} - 1$$

and

$$V = e^{\beta\Delta}\left[\frac{1 - e^{-\beta\Delta}}{1 - e^{-\beta(1-\Delta)}}\right] .$$

Furthermore, in free boundary conditions (or for those discussed in the previous paragraph), the measure is strong-FKG with respect to the ordering $\emptyset \prec [white] \prec [black]$. Finally, these measures are separately increasing in the parameters U and V.

Proof. The relationship between the parameters follows from a thorough once-over of all the steps in the derivation. Faithfulness of the black and white measure in any finite volume setups described so far is clear: Sites in different ω-components are independent, sites that are connected by black bonds are in the same state and sites within the same ω-component that are not connected by black bonds either agree or disagree by 2 with equal probability. In the black-wired problems, corresponding to a particular value at the boundary, the black component of the boundary is assigned the boundary value.

General measures with boundary conditions coming from the spin system are handled in the obvious way: The free boundary sites may be dismissed from consideration and the remaining sites are divided into four separate components according to their assigned spin values. Each of these four components are considered to be "already" connected by black bonds. The weights of the corresponding graphical measure are determined in accordance with the formula in Eq. (3.6) with the provisos that:

(1) There can be no black connections between any of above-mentioned four boundary components. (These four may or may not be figured into the counting of $c(\eta)$ since this will factor out in either case.)

(2) For the white bonds, the boundary components corresponding to 0 and to 2 are here considered to be the same and similarly for $+1$ and -1. No white connections are allowed between the $(0,2)$ boundary component and the $(+1,-1)$ boundary component. (These two white components may or may not be figured into the counting of $c(\omega)$.)

To prove the FKG property, we need only verify the lattice condition for the weights. Notice, that in Eq. (3.6b) the weights have been factored into a product of terms each of which individually satisfies the lattice condition. It turns out, as is easily seen, that for (ω_1,η_1) and (ω_2,η_2) satisfying $\eta_i \subset \omega_i$, we get $(\omega_1,\eta_1)\vee(\omega_2,\eta_2)=(\omega_1\vee\omega_2, \eta_1\vee\eta_2)$ and similarly for $(\omega_1,\eta_1)\wedge(\omega_2,\eta_2)$. The FKG property follows immediately.

Finally, to demonstrate the monotonicity in U and V, observe that if $U'\geqslant U$ and $V'\geqslant V$ the weights for the system with parameters U' and V' may be written

$$W_{BW}^{AT}(\omega,\eta)' \propto W_{BW}^{AT}(\omega,\eta)\left(\frac{U'}{U}\right)^{N(\omega)}\left(\frac{V'}{V}\right)^{N(\eta)} \tag{3.7}$$

and the coefficient of $W_{BW}^{AT}(\omega,\eta)$ is seen to be an increasing function. This gives us the desired monotonicity. □

Of additional interest is the following:

Proposition 3.2. The grey measures satisfy the strong FKG property. In particular, if $\mu_G^{AT;*}(-)$ is the grey measure defined by integrating out the black and white degrees of freedom with (black and white) boundary conditions $*$, then $\mu_G^{AT;*}(-)$ is strong FKG. Finally, if $*' \succ *$,

$$\mu_G^{AT;*'}(-) \underset{\text{FKG}}{\geqslant} \mu_G^{AT;*}(-).$$

Furthermore, we may define the AT-black measures, $\mu_B^{AT;*}(-)$ by integrating out the white components: $\mu_B^{AT;*}(\eta)=\sum_{\omega:\eta\subset\omega}\mu_{BW}^{AT;*}(\omega,\eta)$. These measures are also strong FKG and satisfy the above sort of dominance relations with respect to ordered $*$'s.

Remark. In fact this proposition follows from hypotheses that are somewhat weaker than those implied by the explicit form of the weights. Furthermore, the above type of result holds in various other contexts that will be needed later. We therefore will prove this proposition in the form of a more general lemma. However, the full content of this lemma are not of immediate importance except that it allows for a smoother ride through Theorem 3.4. In this regard, the bottom line is that in finite volume, the maximal grey FKG measure is the one obtained from the reduction of the black-wired boundary conditions. The lemma and its proof have been relegated to Section B.3 of Appendix B.

Proof of Proposition 3.2. Follows from Lemma B.4.

The principal result of this subsection can now be readily derived:

Theorem 3.3. Consider the Ashkin–Teller model with $0 \leqslant \Delta \leqslant 1$ at inverse temperature β. Let $g = g(\beta, \Delta)$ and $a = a(\beta, \Delta)$ be as described and, for a finite box $\Lambda \subset \mathbb{Z}^d$ let $\mu^{AT}_{BW;(g,a)}(-|\Lambda, w)$ denote the AT black and white random cluster measures at these parameter values in the finite box Λ with black-wired boundary conditions on $\partial\Lambda$. Then

$$\mu^{AT;w}_{BW;(g,a)}(-) = \lim_{\Lambda \nearrow \mathbb{Z}^d} \mu^{AT}_{BW;(g,a)}(-|\Lambda, w)$$

exists (and is unique and translation invariant) for any increasing sequence of boxes that exhaust the lattice. For these problems, let us define "percolation" to mean that the probability that the origin is connected to the boundary does not tend to zero as $\Lambda \nearrow \mathbb{Z}^d$. Then the absence of percolation by grey (black and white) bonds, in the black-wired system is the necessary and sufficient condition for unicity of the Gibbs state in the spin system. Furthermore, percolation of black bonds in the black-wired setup is the necessary and sufficient condition for the low-temperature phase (as characterized by the positivity of the spontaneous magnetization). If β is large enough while $\beta\Delta$ is not too large, there is no spontaneous magnetization but there are (at least) two Gibbs states that are characterized by an abundance of 2's and 0's over $+1$'s and -1's and vice versa. In these states, the density of 2's equals the density of 0's and the density of $+1$'s equals the density of -1's. On the other hand, for any fixed $\Delta > 0$, if β is large enough, there is a low-temperature magnetized phase corresponding to (at least) four distinct states. Thus, at least for some values of Δ there is an intermediate phase. Finally, the order parameters for the associated phases defined via the excess of 0's and 2's over $+1$'s and -1's and the excess of 0's over 2's in an appropriate state are precisely the above-mentioned percolation densities (which are well defined).

Remark. The existence of this intermediate phase was first proposed in [23] and established, by rigorous methods, in [22].

Proof. Certain portions of proof follow the methods used in [12] where corresponding statements were established for the Potts/FK system. Notwithstanding, we will provide a complete albeit abridged proof. If $\Lambda_1 \subset \Lambda_2$, the measure $\mu^{AT}_{BW;(g,a)}(-|\Lambda_1, w)$ dominates, in the sense of FKG, the measure $\mu^{AT}_{BW;(g,a)}(-|\Lambda_2, w)$ restricted to Λ_1. Thus, the average of any local function that is FKG increasing converges along any nested sequence of boxes that exhaust $\mathbb{Z}^d$. By comparison to an appropriate subsequence of any standard sequence of boxes, e.g. increasing hypercubes centered at the origin, it is seen that the ultimate answer for this average is, in fact, independent of how $\Lambda \nearrow \mathbb{Z}^d$. Since any local function can be expressed as combinations of increasing functions, this establishes, unambiguously, the existence of a limiting measure for these boundary conditions. This measure will be referred to as the *black-wired* measure. By examining expectations of local functions in shifted boxes of any standard sequence, translation invariance is

established and similarly for the various lattice symmetries (and similarly for other lattices, etc.).

In finite volume, any given site must be disconnected from the boundary, connected to the boundary by a black path or connected to the boundary in such a way that any connecting path uses at least one white bond. In the infinite volume limit, these probabilities converge to well defined densities; let us denote the second by the black percolation density and the sum of the last two by the grey percolation density. We say there is grey or black percolation if the corresponding density is positive.

Suppose, then, that there is black percolation in the black-wired state. Then, clearly, there are (at least) four distinct extremal Gibbs states depending on our identification of the limiting boundary component. Consider a finite volume spin system with each boundary spin taking on one of the four values. It is not hard to see that the excess density of 0's over 2's, the order parameter for the low-temperature phase, is the percentage of sites black-connected to the 0-component of the boundary minus the percentage of sites black-connected to the 2-component of the boundary. This does not exceed the positive term alone which is in turn optimized by setting all the boundary spins to zero, i.e. the wired state. But here the aforementioned inequality saturates. Evidently, the black percolation density in the black-wired state is exactly the order parameter of this phase.

Next, suppose that there is grey percolation but no black percolation in the black-wired state. Then, with the same identification of the boundary component as above, the grey percolation density is the excess density of 0's and 2's and clearly, the wired state is just the one that optimizes this commodity. However each site in the boundary component that is white-connected to the boundary is equally likely to be 0 or 2. Hence, the region where there is grey percolation without black percolation represents the intermediate phase.

By standard arguments, it is possible to show that for any fixed $\Delta > 0$ there is magnetization for β sufficiently large and a high-temperature phase for β sufficiently small. (This will do for the time being; some reasonable bounds will emerge from our later analysis.) Let us now establish the existence of a region where there is grey percolation but no black percolation – our intermediate phase.

As argued previously, the measure is separately increasing in U and V and therefore dominates its $V \to 0$ limit. However, this limiting measure assigns zero weight to any configuration with black bonds, hence $q^{c(\eta)}$ is a constant and what emerges is the random cluster version of the Ising magnet at the effective inverse temperature $\beta(1-\Delta)$. Thus, for any V, the grey measure FKG dominates the usual Ising random cluster measure at parameter $p_{g,a} = 1 - e^{-\beta(1-\Delta)}$:

$$\mu^{AT}_{G;(g,a)}(-) \underset{\text{FKG}}{\geqslant} \mu^{FK}_{q=2,\,p_{g,a}}(-)\,. \tag{3.8}$$

In particular, there will be grey percolation if $\beta(1-\Delta) > \beta_c^{\text{Ising}}$. On the other hand, the measure is dominated by its $U \to \infty$ limit which forces every bond to be black or white. The $q^{c(\omega)}$ drops out of the picture and, as far as the blacks are concerned, we

have another effective Ising random cluster problem here at the density parameter a. This may be expressed:

$$\mu^{AT}_{B;(g,a)}(-) \underset{\text{FKG}}{\leqslant} \mu^{FK}_{q=2,a}(-)\,. \tag{3.9}$$

So if $a < 1 - e^{-\beta_c^{\text{Ising}}} \equiv p_c^{\text{Ising}}$ then there is no percolation of blacks.

Thus, all we need is to satisfy $p_{g,a} > p_c^{\text{Ising}} > a$. However, $a \to 0$ as $\Delta \to 0$ while $p_{g,a}$ increases to $1-e^{-\beta}$. It follows that whenever $\beta > \beta_c^{\text{Ising}}$, we are in the intermediate phase for all Δ sufficiently small.

Finally, let us show that when there is no grey percolation in the wired state, the graphical measure has a unique limit. Using straightforward arguments based on Proposition 3.1 this result will carry over to the desired uniqueness statement in the spin system. Denoting the free boundary condition measures in a finite box Λ by $\mu^{AT}_{BW;(g,a)}(-|\Lambda, f)$, we have a similar sort of volume dominance as in the wired case but pointing in the opposite direction. Thus we arrive at an unambiguous limiting measure that we will denote by $\mu^{AT;f}_{BW;(g,a)}(-)$. Now let $\tilde{\Lambda}$ denote a large finite volume and let $\Lambda \subset \tilde{\Lambda}$. Let $*$ denote any boundary condition on $\tilde{\Lambda}$ and consider the resultant measure restricted to Λ. If we condition on the event that there is no connection between Λ and $\partial\tilde{\Lambda}$, it can be shown that the resulting measure is above (in the sense of FKG) the measure $\mu^{AT}_{BW;(g,a)}(-|\Lambda, f)$ and below the measure $\mu^{AT}_{BW;(g,a)}(-|\tilde{\Lambda}, f)$ as restricted to Λ. Notice that as $\tilde{\Lambda} \nearrow \mathbb{Z}^d$ and $\Lambda \nearrow \mathbb{Z}^d$, these latter measures agree. Now if there is no grey percolation, in the black-wired state, the probability of a connection between Λ and $\partial\tilde{\Lambda}$ tends to zero regardless of the boundary condition * because this is true even with the best boundary conditions on $\tilde{\Lambda}$. Evidently, when there is no percolation, all of the limiting graphical measures agree with $\mu^{AT;f}_{BW;(g,a)}(-)$.

Uniqueness of the Gibbs measure in the spin system now follows from the fact that the average of any local observable in any thermodynamically increasing sequence of finite volume states is independent of the sequence and equals the corresponding average in the infinite volume free state. All of the stated claims have now been established. □

Remark. In the region $\Delta \ll 1$, it appears that the antiferromagnetic aspects of the this Hamiltonian has rendered the multicolored representation of the previous section almost useless for the analysis of the transition into the low-temperature phase. Indeed, if $\Delta = 0$, we get an infinite temperature Ising system on the graph provided by the grey (as in white) clusters. If this is sufficiently dense ($\beta \gg 1$) and the dimension is greater than two, it is fairly certain that the plus-spins (i.e. the 0's) percolate which would imply percolation of the blue bonds. Hence this scenario is likely for β large and $\beta\Delta$ small. In particular, this occurs in the limit $\Delta = 0$, $\beta \to \infty$ by the result of [24]. In any case, blue percolation occurs on the Bethe lattice before the onset of the low-temperature phase [19].

This finishes our discussion of the statistical mechanics of the standard AT model for this region of parameter space. Before we get to a discussion of the algorithms, let

us describe some generalizations of the AT model and the associated representation. The representations and cluster algorithms for all these spin systems differ only in the values of certain parameters. As a side benefit, this will allow, via comparison inequalities, improvements in the estimates for the various transition temperatures.

The generalization of the AT model is immediate from the form of the graphical weights in Eq. (3.6): Clearly, we may replace the 2's by arbitrary positive numbers. Thus, for r and s positive, we can define the generalized AT-random cluster models at density parameters $P=(g,a)$ and geometric parameters $Q=(r,s)$ by

$$\mu^{AT}_{Q,P}(\omega,\eta) \equiv \mu^{AT}_{BW;Q,P}(\omega,\eta) \propto B_g(\omega) r^{c(\omega)} B_a(\eta) s^{c(\eta)} \chi_{\eta\subset\omega}\,, \tag{3.10}$$

where, if unadorned, it will henceforth be assumed that the measure refers to the black and white problem. (Of course, the above formula is only for finite volumes where some additional fuss should be made about boundary conditions. Infinite volume measures are then extracted through weak limits.) If both r and s are integers exceeding one, this is the graphical representation of a genuine spin system. Indeed, this is just a $q=rs$-state spin model, with an additive structure satisfying

$$-1 = \mathscr{E}_{0,0} \leqslant -(1-\Delta) = \mathscr{E}_{0,s} = \cdots = \mathscr{E}_{0,(r-1)s} \leqslant 0 = \mathscr{E}_{0,\alpha} \tag{3.11}$$

where α is any spin state that is not a "multiple" of s. A restricted version of this model ($s=2$ in a different region of parameter space) was introduced in [9] and is known as the cubic model. The full model treated here and in the next subsection was described in [10] and christened the (N_α, N_β) models. This nomenclature does not seem to be in common use and these systems are usually referred to as the cubic models or generalized AT models, a convention to which we will adhere.

Needless to say, nothing beyond the elementary FKG properties of the black and white representation were used in any of the proofs of this subsection. These are easily established for the above measures and we get, for free,

Theorem 3.4. For $r\geqslant 1$ and $s\geqslant 1$ all of the results stated in Proposition 3.1 and 3.2 and Theorem 3.3 with the exception of the faithfulness clause of Proposition 3.1 hold for the generalized AT-random cluster measures $\mu^{AT}_{BW;P,Q}(-)$ provided that various 2's and 4's are replaced by r's, s's and rs's when appropriate. For integers $r\geqslant 2$ and $s\geqslant 2$ these graphical problems are faithful representations of the rs-state spin system (generalized AT model) described in Eq. (3.11). In particular, all of these systems have intermediate phases.

Proof. Follows from the existing argument mutatis mutandis. □

Remark. If $r=1$ and $s>1$ is an integer, it is clear that the generalized random cluster problem is the graphical representation for the annealed bond-diluted s-state Potts model; the P-parameters are determined by $a=1-e^{-\beta}$ and $g=1-e^{-\beta\lambda}$ where λ is the bond chemical potential. As was demonstrated in [25], this is equivalent to a

uniform s-state Potts model.[4] Here the derivation is even simpler: The black measure is obtained by summing the weights of all the configurations ω that contain a given η:

$$W_{B;(r=1,s)P}{}^{AT} \propto s^{c(\eta)} \left[\frac{a}{1-a}\right]^{N(\eta)} \sum_{\omega \supset \eta} \left[\frac{g(1-a)}{1-g}\right]^{N(\omega)} = s^{c(\eta)} \left[\frac{ag}{1-ag}\right]^{N(\eta)} \tag{3.12a}$$

which is exactly the weights of the FK random cluster measure at parameter p given by

$$p = ag\,. \tag{3.12b}$$

As we shall see shortly, this will serve a useful function. The models with $s=1$ are also (thermodynamically) equivalent to the r-state Potts models and will also serve a useful function. However in such systems, the physical interpretation is not so clear.

In [27,12], a certain class of *comparison* inequalities for the random cluster models were derived that are easily be extended to the AT-random cluster systems.

Proposition 3.5. Consider two AT-random cluster measures $\mu^{AT;}_{C;Q_1,P_1}(-)$ and $\mu^{AT;}_{C;Q_2,P_2}(-)$ defined either in finite volume with the same boundary conditions or constructed in infinite volume from the same sequence of boundary conditions and where C denotes, B, G, or BW. Consider the quantities $U(a,g)$ and $V(a,g)$ as defined in Eq. (3.6b) and denote, e.g. $U_1 \equiv U(a_1,g_1)$. Then, if $U_1 \geqslant U_2$ and $V_1 \geqslant V_2$ while $r_1 \leqslant r_2$ and $s_1 \leqslant s_2$, we have

$$\mu^{AT}_{C;Q_1,P_1}(-) \underset{\text{FKG}}{\geqslant} \mu^{AT}_{C;Q_2,P_2}(-)\,.$$

On the other hand, if $U_1/r_1 \leqslant U_2/r_2$ and $V_1/s_1 \leqslant V_2/s_2$, while $r_1 \leqslant r_2$ and $s_1 \leqslant s_2$, we have

$$\mu^{AT}_{C;Q_1,P_1}(-) \underset{\text{FKG}}{\leqslant} \mu^{AT}_{C;Q_2,P_2}(-)\,.$$

Proof. Writing the AT-weights as in Eq. (3.6), it is noted that the geometric factors, $c(\omega)$ and $c(\eta)$ are decreasing functions of the configuration. Thus, e.g. for the black and white,

$$\begin{aligned} W_{Q_2,P_2}{}^{AT}(\omega,\eta) &\propto U_2^{N(\omega)} r_2^{c(\omega)} V_2^{N(\eta)} s_2^{c(\eta)} \chi_{\eta \subset \omega} \\ &= W_{Q_1,P_1}{}^{AT}(\omega,\eta) \left(\frac{U_2}{U_1}\right)^{N(\omega)} \left(\frac{r_2}{r_1}\right)^{c(\omega)} \left(\frac{V_2}{V_1}\right)^{N(\eta)} \left(\frac{s_2}{s_1}\right)^{c(\eta)}. \end{aligned} \tag{3.13}$$

Hence if $U_1 \geqslant U_2$, $V_1 \geqslant V_2$ $r_1 \leqslant r_2$ and $s_1 \leqslant s_2$, the weights of the second measure have been expressed as the weights of the first measure multiplied by a decreasing function

[4] The existence of a relationship was noted earlier. In [26], a complicated formula related the bond fugacity, bond concentration and temperature of the annealed system to the temperature and energy density of the corresponding pure system. However, it seems that this formula is parts of Eq.(3.12b) – which is Eq.(1.4b) in [25] – and Equation (2.6) in [8] tangled together. As is explicitly seen in Eq.(3.12b), the effective temperature can be calculated from the actual temperature and the bond fugacity without knowing the energy density as a function of temperature in the pure system.

which, for the black and white case, gives us the first domination. As an elementary consequence of the considerations in Lemma B.4, this argument carries us through for the grey and black measures as well. For the dominations in the other direction, we use $c(\omega) = \ell(\omega) - N(\omega) +$ [const.] where $\ell(\omega)$ is the number of independent loops and similarly for η. Notice that $\ell(\omega)$ and $\ell(\eta)$ are increasing functions. Thus we obtain, for the black and white,

$$W_{Q_1,P_1}{}^{AT}(\omega,\eta) \propto \left(\frac{U_1}{r_1}\right)^{N(\omega)} r_1^{\ell(\omega)} \left(\frac{V_1}{s_1}\right)^{N(\eta)} s_1^{\ell(\eta)}$$

$$= W_{Q_2,P_2}{}^{AT} \left(\frac{U_1 r_2}{U_2 r_1}\right)^{N(\omega)} \left(\frac{r_1}{r_2}\right)^{\ell(\omega)} \left(\frac{V_1 s_2}{V_2 s_1}\right)^{N(\eta)} \left(\frac{s_1}{s_2}\right)^{\ell(\eta)} \tag{3.14}$$

which implies the second set of comparison inequalities. □

As was alluded to above, if either s or r is one, the model collapses into the Potts (or random cluster) model in the remaining variable. Proposition 3.5 then gives us

Corollary. Let $p_c(q)$ denote the percolation threshold in the random cluster models with parameter q. Consider the general AT-random cluster models as described with parameters g, a, r, and s and, for simplicity, assume that r and s are not less than one. Then, if $ga < p_c(s)$ there is no black percolation, if $g < p_c(r)$, there is high temperature behavior while if $ga/[g + r(1-g)] > p_c(s)$ the system has black percolation (positive spontaneous magnetization) and it has grey percolation (implying multiple phases) if $[gs - ga(s-1)]/[s - ga(s-1)] > p_c(r)$.

Proof. The first case is an immediate consequence of Proposition 3.5 and the derivation in Eq. (3.12) – set $r = 1$ to get the bounding measure. Let us explicitly do the last case. Writing the weights in the form of Eq. (3.14):

$$W_{G;Q,P}^{AT} \propto \left[\frac{U}{r}\right]^{N(\omega)} r^{\ell(\omega)} \sum_{\eta \subset \omega} \left[\frac{V}{s}\right]^{N(\eta)} s^{\ell(\eta)}. \tag{3.15}$$

This dominates the measure whose weights are defined as above but with $s^{\ell(\omega)}$ set to one. For the latter weights, the sum may be performed explicitly and the result is proportional to $r^{c(\omega)}[U(1+V/s)]^{N(\omega)}$. This is the r-state Potts model at the stated value of parameter. The other cases follow similar arguments. □

Remark. Notice that the appropriate upper and lower bounds in terms of the s-state or r-state Potts models become exact as we approach the phase boundaries. Of particular interest is the point $\Delta = 0$, $T = 0$ where the statistical mechanics is ambiguous. This is obvious if we examine the approaches $\Delta = 0$, $T \to 0$ and $T = 0$, $\Delta \to 0$ respectively; in both cases, the grey bonds are saturated but in the former approach, they are all white and in the latter, they are all black. As will become evident, this point on the

phase diagram is a K-point, i.e. it embodies an entire statistical mechanics problem where the parameter is determined by the angle of approach. For the usual AT-models, this K-point is the Ising magnet and for the generalizations, it the s-state Potts model. Indeed, let us write $\beta\Delta = \alpha$ and let $\beta \to \infty$ and $\Delta \to 0$ in such a way that α tends to a finite constant. Then, our upper and lower bounding measures agree with the naive limit which is $g \to 1$ and

$$a(\alpha) = 1 - e^{-\alpha}/1 - e^{-\beta} \to 1 - e^{-\alpha}. \tag{3.16}$$

With g saturating at one, the only action is in terms of the black bonds which play the role of the usual s-state random cluster model at $p = 1 - e^{-\alpha}$ (as is the case in the coinciding domination bounds in this limit). In this way the limiting slope of the magnetization phase boundary is established exactly and with complete rigor.

Let us note, in closing, that schemes for the construction of new graphical models need not stop with the usual random cluster weights for the "grey" and "black" bonds. Indeed, if W_1 and W_2 are some other type of graphical weights – preferably with the FKG property – we can always define $W_{12}(\omega, \eta) = W_1(\omega)W_2(\eta)\chi_{\eta \subset \omega}$. Furthermore, the ω and the η can have compound structures themselves. Clearly, if W_1 and W_2 correspond to spin systems, so does W_{12} but we have not yet performed a systematic study of just which systems can be reached by these constructions. But, for an example, if W_1 is the three state Potts model and W_2 is the Ashkin–Teller model then the combination is a twelve state model with $\mathscr{E}_{0,0} \leqslant \mathscr{E}_{0,6} \leqslant \mathscr{E}_{0\pm3} \leqslant \mathscr{E}_{0\pm1} = \cdots = \mathscr{E}_{0\pm5}$. Obviously such a system will have two intermediate phases the existence of which could be readily established by graphical methods. These sorts of generalizations will be pursued at some future point.

3.2.1. *Swendsen–Wang algorithms*

The algorithms suggested by the black and white representation are almost inevitable. Although these are covered by the formalism in Appendix A, the crucial point (which cannot be addressed in so general a context) is that here the "spin moves" can be performed in time proportional to the volume.

3.2.1.1. Description and detailed balance. Consider an AT-model with parameters $Q = (r, s)$ and $P = (g, a)$. Starting from a black and white bond configuration, each grey cluster is independently assigned an integer $1, 2, \ldots, r$. All of the white bonds can now be erased leaving a collection of black connected clusters. Each black cluster is independently assigned an integer $1, 2, \ldots, s$ and the resulting spin value, which is constant within each black cluster, is given by the product of the two integers that were assigned to the spin. This defines the updated spin configuration. Bonds are now placed as follows: Between every pair of neighboring spins that agree, a black bond is placed with probability ga. Among those pairs where the black bonds have failed or among those pairs where the spins agree modulo s, white bonds are placed with probability $[g(1-a)]/[1-ga]$. An elementary calculation or (more difficult) a detailed

look at Appendix A with the Hamiltonian written as

$$\mathscr{H}(\underline{\sigma}) = \sum_{\langle i,j \rangle} \mathscr{E}_{0,s}\chi(\sigma_i = \sigma_j \bmod s) + (\mathscr{E}_{0,0} - \mathscr{E}_{0,s})\chi(\sigma_i = \sigma_j) \tag{3.17}$$

establishes detailed balance via the appropriate ES weights.

3.3. The orthodox ferromagnetic region

Now, finally, to the Orthodox Ferromagnetic Region, $2 \geqslant \Delta \geqslant 1$. At first glance, this would seem to be a standard ferromagnetic phase transition – less interesting than in the unorthodox region. However in two-dimensions, presumably, the phase boundary is a self-dual line that represents a line of continuously varying exponents. This provides an incentive for the development of graphical representations and cluster algorithms for this regime. It turns out that what follows is closely related to the cluster method proposed in [28]; indeed the SW-type algorithms here and in [28] are nearly identical. However our derivation will be quite different (and somewhat more straightforward) leading to a closed form FK-style expression for the weights of the graphical representation. This in turn allows us to establish rigorously that the graphical representation "captures the basic excitations of the model" – i.e. a percolation phenomenon characterizes the low-temperature phase – as was indicated by the success of the simulations in [28].

The above-mentioned duality is manifest in the graphical representation; indeed, it may be derived for the graphical representation itself. Furthermore, the derivation applies to the generalized AT (cubic) models, in both regions, without the restriction to integer values of the parameters r and s. For the spin systems, duality was derived in [10,29] by standardized machinery. The graphical method is more transparent and, cf. Section 4, allows various results to be established with mathematical rigor. However, these specialized issues are peripheral to the central objectives of this work and hence the duality relations will be derived in Section B.1 of Appendix B.

In the orthodox region, $2 \geqslant \Delta \geqslant 1$, one anticipates (and here we prove, cf. Theorem 3.7 for a precise statement) that there are no ordering transitions other than the ferromagnetic one. Thus, the general representation from Section 2 will be susceptible to a "false percolation transition". In particular, it seems that this representation corresponds to the "naive SW option" discussed in Section 1) of [28] which indeed turned out to be impractical for numerical simulations. We therefore turn to the Ising representation of this system. Here, each spin is written in double Ising form $\sigma_i = (\kappa_i, \tau_i)$; $\kappa_i = \pm 1$, $\tau_i = \pm 1$. The correspondence is $0 = (+,+)$, $1 = (+,-)$, $-1 = (-,+)$ and $2 = (-,-)$. Writing

$$\beta\mathscr{H} = -\sum_{\langle i,j \rangle} [K_\kappa \kappa_i \kappa_j + K_\tau \tau_i \tau_j + L\kappa_i \kappa_j \tau_i \tau_j], \tag{3.18}$$

the symmetric cases correspond to $K_\kappa = K_\tau \equiv K$ and the relation to our previous notation is $L = \frac{1}{4}\beta(2 - \Delta)$ and $K = \frac{1}{4}\beta\Delta$.

The graphical representation follows immediately by writing

$$-\beta\mathscr{H} = \sum_{\langle i,j\rangle} K[2\delta_{\kappa_i,\kappa_j} - 1 + 2\delta_{\tau_i,\tau_j} - 1] + L[(2\delta_{\kappa_i,\kappa_j} - 1)(2\delta_{\tau_i,\tau_j} - 1)]$$
$$= \sum_{\langle i,j\rangle} \beta(\Delta - 1)[\delta_{\kappa_i,\kappa_j} + \delta_{\tau_i,\tau_j}] + \beta(2 - \Delta)\delta_{\kappa_i,\kappa_j}\delta_{\tau_i,\tau_j} + \text{const.} \tag{3.19}$$

We may visualize the system as having a τ-layer of spins one unit "below" the κ-layer and the partition function is expanded in the usual fashion. Bonds can occur between neighboring pairs of κ-spins with density parameter $p_1 = 1 - e^{-\beta(\Delta-1)}$ tying these spins together in the same state and similarly for pairs of τ-spins. In addition, there are *double bonds* that have the same effect as the simultaneous occurrence of a τ-bond and a κ-bond. Such objects occur with density parameter $p_2 = 1 - e^{-\beta(2-\Delta)}$. A given pair of spins may be tied by either or both mechanisms; the presence or absence of one type does not exclude nor imply the presence of absence of the other. Any collection of these sorts of bonds divides both the κ and τ layer into connected components, of which there are c_κ and c_τ respectively. If $\omega = (\omega_\kappa, \omega_\tau, \omega_{\kappa\tau})$ is a configuration of these three types of objects, there are $2^{c_\kappa(\omega)}2^{c_\tau(\omega)}$ spin configurations consistent with this configuration. (Note that c_κ actually depends only on ω_κ and $\omega_{\kappa\tau}$ and similarly for c_τ with $\kappa \leftrightarrow \tau$). Evidently, on a finite lattice the weight of a configuration ω is given by

$$Y^{AT}(\omega) = B_{p_1}(\omega_\kappa)B_{p_1}(\omega_\tau)B_{p_2}(\omega_{\kappa\tau})2^{c_\kappa(\omega)}2^{c_\tau(\omega)} \tag{3.20}$$

where $B_{p_1}(\omega_\kappa)$, $B_{p_1}(\omega_\tau)$ and $B_{p_2}(\omega_{\kappa\tau})$ are the usual Bernoulli factors associated with the separate configurations of κ-bonds, τ-bonds and $\kappa\tau$-double bonds.

We remark that for a general Hamiltonian of the form given in Eq. (3.19), provided that the coefficients of all the Kronecker δ's functions are kept positive, there is no need to insist that the coefficients of $\delta_{\kappa_i,\kappa_j}$ and δ_{τ_i,τ_j} are the identical. In the future, we will not do so, and we will name the associated density parameters p_κ and p_τ and use $p_{\kappa\tau} \equiv p_2$. Furthermore, there is no compelling reason that the κ's and τ's have to be 2-state Potts variables. We will replace the 2's in Eq. (3.20) by an r and an s. It is noted that these generalizations tack directly onto the generalizations discussed in the previous section forming a single phase diagram.

The first proposition of this subsection demonstrates the utility of the graphical representation in Eq. (3.20) and its various generalizations:

Proposition 3.6. Consider an $r \times s$ state model with a Hamiltonian of the form described in the last line of Eq. (3.19) with all coefficients positive. Then, the analog of the weights described in Eq. (3.20), $Y^{AT}_{Q,P}(-)$ with $Q = (r,s)$ and $P = (p_\kappa, p_\tau, p_{\kappa\tau})$ defines a measure that faithfully describes this model. Furthermore, these measures have the strong FKG property under the ordering $\omega \succ \eta$ implies $\omega_\kappa \succ \eta_\kappa$ and $\omega_\tau \succ \eta_\tau$ and $\omega_{\kappa\tau} \succ \eta_{\kappa\tau}$ (not necessarily strict).

Proof. To establish the FKG property, it is enough to verify the lattice condition for the weights $Y^{AT}_{Q,P}(-)$ which are now written as

$$Y^{AT}_{Q,P}(\omega) = s^{c_\kappa(\omega)} r^{c_\tau(\omega)} B_{p_\kappa}(\omega_\kappa) B_{p_\tau}(\omega_\tau) B_{p_{\kappa\tau}}(\omega_{\kappa\tau}) . \tag{3.21}$$

Thus, it is sufficient to separately establish that

$$c_\kappa(\omega \wedge \eta) + c_\kappa(\omega \vee \eta) \geqslant c_\kappa(\omega) + c_\kappa(\eta) \tag{3.22}$$

and similarly for $c_\tau(-)$. We have now, in essence, reduced the problem to the familiar one for the FK representation of the Potts models – all that is involved concerns single layers, one at a time, consisting of sites with bonds between certain pairs. It seems clear that almost any derivation for the Potts model is applicable in this case; for completeness, we will recapitulate the proof in [12].

Writing $\zeta = \omega \wedge \eta$, the desired inequality reads

$$c_\kappa(\omega \vee \eta) - c_\kappa(\eta) \geqslant c_\kappa(\omega \vee \zeta) - c_\kappa(\zeta) . \tag{3.23}$$

It is claimed that Eq. (3.23) holds for any ω and $\eta \succ \zeta$ for the simple reason that for fixed ω, the left-hand side is an increasing function of η. If ω contains only one object, i.e. it is just one κ-bond or just one double bond that connects the sites i and j, we get that $c_\kappa(\omega \vee \eta) - c_\kappa(\eta)$ is zero if i and j are connected in η and negative one otherwise. This is clearly increasing. If the (simple) statement is true for any ω containing $k-1$ objects, let $\omega' = \omega \vee b$ denote a configuration consisting of k objects. Then

$$c_\kappa(\omega' \vee \eta) - c_\kappa(\eta) = [c_\kappa(\omega \vee b \vee \eta) - c_\kappa(b \vee \eta)] + [c_\kappa(b \vee \eta) - c_\kappa(\eta)] \tag{3.24}$$

is the sum of two increasing functions. This completes the proof of the FKG property.

The graphical representation is faithful for the usual reasons: the expectations of local observables may be expressed as the sums and differences of various connectivity properties between subsets of the set of sites on which the relevant spins reside. □

As an immediate consequence, we obtain:

Theorem 3.7. For the AT models as described in Proposition 3.6, the phase structure of the model is characterized by the percolation properties of the graphical representation. In particular, the Gibbs state of the spin system is unique if and only if there is no percolation, in either layer, in the limiting wired state. If $s = r$ and $p_\kappa = p_\tau$, there is a single ordering transition as the temperature is varied. However if, e.g. p_κ is sufficiently large and p_τ and $p_{\kappa\tau}$ are sufficiently small there will be κ ordering without τ ordering while if all parameters are close to one, there is percolation in both layers. Thus, for certain values of the parameters, there is an intermediate phase. In all cases, the relevant percolation density corresponds to the order parameter for the appropriate phase.

Remark. For the (asymmetric) 4-state Ashkin–Teller model the intermediate phase in this regime was established in [22]. The method also used correlation inequalities but these were of the GKS-type which, by and large, are restricted to Ising systems.

Proof. The argument connecting unicity of Gibbs states to absence of percolation is the same as was used in Theorem 3.3. When there is percolation, in only one or in both layers, the relationship between the various percolation probabilities and the appropriate order parameters is obvious and need not be made explicit. Under the conditions of complete symmetry between the layers, it is clear that there is percolation in the τ-layer if there is percolation in the κ-layer.

The existence of intermediate phases in asymmetric cases is a consequence of the following dominations. Let us denote these generalized Ashkin–Teller graphical measures by $v^{AT}_{Q,P}(-)$. We may consider the restriction of this measure to (events in) the κ layer, $v^{AT}_{Q,P}(-)_{||\kappa}$ and similarly for the τ-layer. Note that for the graphical representation (κ–bonds *or* the top half of double bonds) the measure $v^{AT}_{Q,P}(-)_{||\kappa}$ is an effective s-state FK measure with complicated correlations. We claim that

$$\mu^{FK}_{s,p_\kappa}(-) \underset{\text{FKG}}{\leqslant} v^{AT}_{Q,P}(-)_{||\kappa} \underset{\text{FKG}}{\leqslant} \mu^{FK}_{s,p^*_\kappa}(-) \tag{3.25}$$

where $\mu^{FK}_{q,p}(-)$ are the usual FK measures and $p^*_\kappa = p_\kappa + p_{\kappa\tau} - p_\kappa p_{\kappa\tau}$. For the above, in finite volume, it is assumed that the κ layer in the AT system has the same boundary conditions as the comparison measures.

The lower bound is completely trivial; $v^{AT}_{Q,P}(-)$ is FKG increasing in all of the "P" parameters, and $\mu^{FK}_{s,p_\kappa}(-)$ is exactly what we get if we set $p_\tau = p_{\kappa\tau} = 0$. On the other hand, whenever we condition $v^{AT}_{Q,P}(-)$ on a positive event, we get an increased measure. Let us condition on the event that all the bonds in the τ-layer are occupied. (For infinite volume problems, where this procedure sounds a little singular, note that it is sufficient to establish the inequalities in finite volume and take limits later.) But, under this condition, the measure in the top layer is seen to be another s-state Potts model of the usual sort: Now all bonds can be either a double bond or a single bond with no interplay between the two types. This gives us an effective s-state random cluster measure with parameter $p_\kappa(1 - p_{\kappa\tau}) + p_{\kappa\tau}(1 - p_\kappa) + p_\kappa p_{\kappa\tau} = p^*_\kappa$. Of course the same set of ideas holds for the restriction to the τ-layer and, if we have $p_\kappa > p_c(s)$ and $p^*_\tau < p_c(r)$, there is percolation in the σ-layer but not in the τ-layer. On the other hand, for all the p's close to one, there is percolation in both layers. All claims have now been established. □

Remark. Without much additional labor, an improvement can be made in the first of the domination inequalities in Eq. (3.25) along the lines of Proposition 3.5. Indeed, it is noted that for these AT measures, there is also an FKG monotonicity in Q: larger Q is worse for fixed p's and larger Q is better for appropriately lowered p's. (Indeed, the right-hand domination may be obtained by setting $r = 1$.) First off, we set $p_\tau = 0$ to get a lower measure. Now, the only forces creating clusters in the τ-layer are the double bonds. Furthermore, as in previous arguments the weights may be rewritten in terms

of the loops resulting in $\mu^{FK}_{q,p}(\omega) \propto B_b(\omega) q^{\ell(\omega)}$ where $b = b(p,q) = p/[p + q(1-p)]$ and $\ell(\omega)$ is the number of independent loops in the configuration. For fixed b, these measures are FKG increasing in q. Back to the AT measures with $p_\tau = 0$, we can write the τ-layer portion of the measure in this form and then, as a lower bound, set $r = 1$. As a result, we obtain

$$\mu^{FK}_{s,p^{**}_\kappa}(-) \underset{\text{FKG}}{\leqslant} \mu^{AT}_{Q,P}(-)_{||\kappa} \tag{3.26}$$

with $p^{**}_\kappa = p_\kappa + b_\tau - p_\kappa b_\tau$ and $b_\tau = b(p_{\kappa\tau}, r)$. Obviously these bounds constitute an improvement over the ones used in Theorem 3.7 (and over those existing in the literature).

3.3.1. *Swendsen–Wang algorithms*

The SW algorithms and the requisite proofs for the systems described in Proposition 3.6 and Theorem 3.7 are straightforward extensions of the standard Potts cases. A brief description and proof sketch is as follows: Starting from a spin configuration, bonds connecting satisfied neighboring pairs of τ (κ) spins are independently placed with probability p_τ (p_κ). Regardless of the outcome of these τ-bond or κ-bond events, a double bond may be (independently) placed with probability $p_{\kappa\tau}$ on any *fully* satisfied neighboring pair of κ and τ spins. The resulting bond configuration defines connected components in the τ and κ layers each of which (boundary conditions permitting) is independently reassigned to be one of the r (s) values with equal probability. This completes a Monte Carlo step. Detailed balance is established, as in other cases, by writing down the weights for an Edwards–Sokal joint measure which in this case is

$$Y_{ES}{}^{AT}(\omega; \sigma, \tau) = B_\kappa(\omega_\kappa) B_\tau(\omega_\tau) B_{\kappa\tau}(\omega_{\kappa\tau}) \Delta(\omega; \underline{\kappa}, \underline{\tau}) \tag{3.27}$$

where $\Delta(\omega; \underline{\kappa}, \underline{\tau})$ is one if the bond-spin configuration is "consistent" (as can be inferred from the above description) and zero otherwise. The remaining details follow exactly the lines of the previous derivations.

An algorithm for all of these systems was also devised in [28] (although only the 4-state models were discussed explicitly) and on the basis of the general considerations in [1] was shown to satisfy detailed balance. Despite the fact that a graphical representation was never actually discussed, as is clear from the "Ising Embedding" derivation in their appendix, the amalgamation of "generalized freezes" is evidently described by the measures $\nu^{AT}_{P,Q}(-)_{||\sigma}$. Returning to the (primitive) Ising version of the Hamiltonian, Eq. (3.18), and letting (τ) denote a configuration in the τ-layer, the idea is to write an effective Hamiltonian for the κ-layer, given by

$$\beta \mathscr{H}_{\text{eff}} = -\sum_{\langle i,j \rangle} J^{(\tau)}_{i,j} \kappa_i \kappa_j \tag{3.28}$$

where $J^{(\tau)}_{i,j} = K_\kappa + L\tau_i\tau_j$ and then the idea is to use ordinary SW dynamics in the κ layer with this effective Hamiltonian. After an update of the κ-layer, the same is applied

to the τ-layer (thereby updating the effective Hamiltonian) and a cycle is completed. Examining the κ move, for fixed configuration $(\underline{\tau})$, suppose that $\tau_i \neq \tau_j$. Then, if $\kappa_i = \kappa_j$ a bond occurs with probability $1 - e^{-2(K-L)}$ which is equal to p_κ. On the other hand, if $\tau_i = \tau_j$, the bond occurs with probability $1 - e^{-2(K+L)}$ which is seen to equal $p_\kappa + p_{\kappa\tau} - p_\kappa p_{\kappa\tau}$. Thus the algorithm is the same as ordinary SW – using the graphical representation featured in this subsection – but alternating between the κ and τ layers and allowing the double bonds to be reset in each half step of the process. Thus, as far as SW simulations are concerned, there is really nothing new in this subsection. However, having our hands on a closed-form expression for the graphical representation has distinct advantages, e.g. Theorem 3.7. Furthermore, one of the stated objectives of [28] was to test for the validity and possible saturation of a Li–Sokal bound in this system. Although we cannot begin to address the question of whether such a bound saturates, the existence of the representation implies, via Theorem A.2; a Li–Sokal bound for these dynamics.

4. First-order transitions

4.1. Reflection positivity

Reflection positivity (RP) was introduced into statistical mechanics in the late 1970s and early 1980s in a variety of contexts. (cf. the review by [30] and references therein.) Of particular interest is the work of [16] where RP was shown to be the ideal technique for establishing discontinuous phase transitions. Recently, it was demonstrated that RP can be combined with graphical expansions of the FK type [31]; here this result will be generalized and further developed. The combination of graphical techniques with reflection positivity allows a simpler proof of the standard large entropy type transitions and further provides a well defined arena in which these results can be generalized. Of course here we will run up against the usual limitations of the RP technique: we must (essentially) confine ourselves to nearest neighbor interactions and in addition we must work on the torus.

In order to keep this work down to a manageable length, rigorous proofs will be provided only for two-dimensional problems. This allows us to use the *diagonal* torus (SST) which cuts down on the number of diagrams that need to be considered. Furthermore, mostly for the purpose of conceptual clarity, we will discuss only the "user friendly" cases featured in Section 2. All of the principal results in this section can be extended to $d > 2$ and to the non-additive cases with suitable modification of the hypotheses. The results that specifically pertain to duality are, of course, special to $d = 2$; these will be set aside as corollaries to the more general results.

Let $\mathscr{T}_N$ denote the two dimensional diagonal torus with N sites. Here the sites have coordinates $i = (i_x, i_y) \in \mathbb{Z}^2$ with the lines $i_x + i_y =$ [const.] identified modulo L, assumed even, and similarly for the lines $i_x - i_y =$ [const.]. (Thus a total of $N = \frac{1}{2}L^2$ sites.) Let

P_0^- be the notation for the pair of lines

$$P_0^- = \{i \in \mathscr{T}_N \mid i_y - i_x = 0 \text{ or } i_y - i_x = L/2\} \tag{4.1}$$

and similarly for P_k^- and P_k^+. It is observed that P_0^- divides the torus into two equal halves that have the sites of P_0^- in common. We will denote these halves by $\mathscr{A}$ and $\mathscr{B}$. Let us assume that we are dealing with a finite system of configurations defined on the sites and bonds (or, occasionally plaquettes, etc) of $\mathscr{T}_N$ in accord with the conventions of the preceding sections. Let Ξ denote the set of all such configurations and let us denote by $\Xi_{\mathscr{A}}$ and $\Xi_{\mathscr{B}}$ the set of configurations that are situated in the two halves of the torus. Let $\vartheta_{P_0^-}$ denote a function that maps each $\eta_{\mathscr{A}}$ in $\Xi_{\mathscr{A}}$ to an $\eta_{\mathscr{B}}$ in $\Xi_{\mathscr{B}}$ and, by abuse of notation, let $\vartheta_{P_0^-}$ also denote the inverse of this function. Such a $\vartheta_{P_0^-}$ will generically be called a *reflection*. If $f = f(\eta_{\mathscr{B}})$ is a real-valued function on $\Xi_{\mathscr{B}}$, we will define $\vartheta_{P_0^-} f = f(\vartheta_{P_0^-}\eta_{\mathscr{A}})$ to be the reflected function and similarly for functions on $\Xi_{\mathscr{A}}$. The starting point is:

Definition. Let $\mathbb{P}$ denote a probability measure on Ξ and $\vartheta_{P_0^*}$, $* = \pm$ a reflection of the type discussed above. Then $\mathbb{P}$ is said to be *reflection positive* with respect to $\vartheta_{P_0^-}$ if for every f and g defined on the configurations $\eta_{\mathscr{B}}$,

(i) $\mathbb{E}(f\vartheta_{P_0^-} f) \geqslant 0$

(ii) $\mathbb{E}(f\vartheta_{P_0^*} g) = E(g\vartheta_{P_0^*} f)$

where $\mathbb{E}(-)$ denotes expectation. For other lines $P_k^{\pm}$ we may have various other $\vartheta_{P_k^+}$ and $\vartheta_{P_k^-}$ and reflection positivity can be defined in a similar fashion. Denoting the collection of all these reflections by ϑ, the probability measure is said to be reflection positive with respect to ϑ if the analogs of (i) and (ii) hold for all the $\vartheta_{P_k^{\pm}}$.

Let us now turn attention to the reflections that are of use in the present context. Recall that in the general multicolored representation, the bonds have to be oriented. Throughout this section, we will assume that the bonds are always oriented in the direction of increasing coordinate. Further, let us refer to bonds that change the spin an equal but opposite amount as *complementary* bonds. In case the change is by $q/2$, the bond is its own complement. (In the non-additive cases, there may be other bonds that are self-complementary.) Complementary configurations (that is the complement of a given bond configuration) will be denoted by affixing a # to whatever symbol describes the original configuration. The reflections that we use are slightly different for the lines P_k^+ and P_k^-. It is clearly sufficient to discuss the reflections $\vartheta_{P_0^+}$ and $\vartheta_{P_0^-}$, let us begin with the latter. Let us define, by further abuse of notation, $\vartheta_{P_0^+}$ as a mapping of the sites and bonds of $\mathscr{A}$ to their mirror image in $\mathscr{B}$ through the line $i_x - i_y = 0$. Writing $\eta_{\mathscr{A}} = (\overline{\omega}_{\mathscr{A}}, \sigma_{\mathscr{A}})$ the reflection $\vartheta_{P_0^-}$, (now defined on configurations in $\mathscr{A}$) consists of the same spin-states and bond values located at the reflected sites. Formally, for $i \in \mathscr{A}$, $\vartheta_{P_0^-}\sigma(\vartheta_{P_0^-} i) = \sigma(i)$ and for $b = \langle i, j\rangle \in \mathscr{A}$ we have $\vartheta_{P_0^-}\overline{\omega}(\vartheta_{P_0^-} b) = \overline{\omega}(b)$. It is observed that this maps consistent configurations into consistent configurations. As for the object $\vartheta_{P_0^+}$, we will also use reflection to define the image of the spin configuration. However,

after a moment's consideration, it becomes clear that we must use the complementary bonds in the reflected positions in order to maintain a consistent configuration. We thus have $\vartheta_{P_0^+}\overline{\omega}(\vartheta_{P_0^+}b)=\overline{\omega}^{\#}(b)$. It is noted that in both cases, the only objects in the reflection plane itself are sites and spins which, in all cases are left invariant.

The following is a generalization of the result in [31]:

Proposition 4.1. Consider the multicolored bond/spin problems defined by the weights in Eqs. (2.14) and (2.15). Then the associated probability measure is reflection positive with respect to all the reflections ϑ as defined above.

Proof. Here we will use an alternative (but equivalent) version of the standard proof which has the advantage that it makes no explicit reference to an underlying Hamiltonian. Starting with $\vartheta_{P_0^-}$, let $\sigma(P_0^-)$ denote any particular configuration of spins in the lines P_0^-. It is not hard to see that for any such $\sigma(P_0^-)$, the conditional distributions in the left and right halves of the torus are independent and identical under the reflection $\vartheta_{P_0^-}$. Indeed, $\mathbb{P}(\eta_{\mathscr{B}}\mid\sigma(P_0^-))$ is just the product of all the fugacity factors for the bonds and the Δ-consistency condition between the bonds and spins. If $\eta_{\mathscr{A}}$ is a configuration, we have the same bonds in $\vartheta_{P_0^-}(\eta_{\mathscr{A}})$ and it is clear that $\Delta(\overline{\omega}_{\mathscr{A}},\sigma_{\mathscr{A}})=1\Leftrightarrow\Delta(\vartheta_{P_0^-}\overline{\omega}_{\mathscr{A}},\vartheta_{P_0^-}\sigma_{\mathscr{A}})=1$. Running through all configurations,

$$\sum_{\eta_{\mathscr{A}}} f(\vartheta_{P_0^-}\eta_{\mathscr{A}})\mathbb{P}(\eta_{\mathscr{A}}\mid\sigma(P_0^-))=\sum_{\eta_{\mathscr{A}}} f(\vartheta_{P_0^-}\eta_{\mathscr{A}})\mathbb{P}(\vartheta_{P_0^-}\eta_{\mathscr{A}}\mid\sigma(P_0^-))$$

$$=\sum_{\eta_{\mathscr{B}}} f(\eta_{\mathscr{B}})\mathbb{P}(\eta_{\mathscr{B}}\mid\sigma(P_0^-))\,. \tag{4.2}$$

Thus, the conditional expectation of $f\vartheta_{P_0^-}f$ is the above quantity squared and hence $f\vartheta_{P_0^-}f$ averages to something positive. The derivation for $\vartheta_{P_0^+}$ is identical after the observation that reversal of the reflected bonds preserves the consistency condition. Similar considerations demonstrate that $\mathbb{E}(g\vartheta_{P_0^\pm}f)=\mathbb{E}(f\vartheta_{P_0^\pm}g)$. □

Remark. On the d-dimensional tori with the usual sort of periodicity, it is clear that the same kinds of results go through: Reflections are through the usual hyperplanes of sites, spins get mapped by pure reflections as do the bonds parallel to the hyperplane while the bonds perpendicular to the hyperplane are replaced by their complements. With this definition, the derivation follows the same course as the above.

The above implies a Cauchy–Schwartz inequality: $\mathbb{E}(g\vartheta_{P_k^\pm}f)\leqslant[\mathbb{E}(f\vartheta_{P_k^\pm}f)]^{1/2}[\mathbb{E}(g\vartheta_{P_k^\pm}g)]^{1/2}$. By repeated applications of the appropriate reflection operations, a local event can be reflected until "it covers the torus". This leads to expressions involving constrained partition functions that, in our case, all turn out to be graphical configurations blanketing the torus. Furthermore, the probability of separated events may be estimated by the product of the estimates corresponding to the individual events; these are known as the *chessboard* estimates, cf. [30, Section 2.4].

For the proofs of discontinuous transitions, we will use the following from [16]:

Lemma 4.2. Let $\mathscr{H}$ be a Hamiltonian of the type described and β the inverse temperature assumed to lie in the range $[\beta_x, \beta_y]$ and let $G_{N,\beta}(-)$ denote the Gibbs/random cluster measure on $\mathscr{T}_N$ induced by the Hamiltonian $\mathscr{H}$ at inverse temperature β. Let b_x and b_y denote two disjoint bond events (i.e. distinctive types of bonds) for some particular bond. Finally let $A \in (\frac{1}{2}, 1]$ and $B \in [0, 1]$ be such that

$$B \leqslant \left[\frac{1}{2} + \sqrt{\frac{1}{2} - \frac{A}{2}}\right]^2$$

and let ε_x, $\varepsilon_y \in (0, \frac{1}{2})$. Suppose that for all $\alpha \in [\alpha_x, \alpha_y]$, and for all $\ell, m \in \mathscr{T}_N$, one has

(i) $G_{N,\beta}(b_x \cup b_y) \geqslant A$,

(ii) $G_{N,\beta}(b_x(m) \cap b_y(\ell)) \leqslant B$,

and, meanwhile,

(iiix) $G_{N,\beta_x}(b_x) > 1 - \varepsilon_x$

and

(iiiy) $G_{N,\beta_y}(b_y) > 1 - \varepsilon_y$.

Further, suppose that the above holds for all N in some sequence $\mathscr{T}_N \nearrow \mathbb{Z}^2$. Then there is a value $\beta_t \in (\beta_x, \beta_y)$ with two distinct (infinite volume) states $G^x_{\beta_t}(-)$ and $G^y_{\beta_t}(-)$. These are characterized, e.g. by the fact that $G^x_{\beta_t}(b_x) \geqslant 1 - \delta$ and $G^y_{\beta_t}(b_y) \geqslant 1 - \delta$, where δ is a particular function of A and B such that $\delta \to 0$ as $A \to 1$ and $B \to 0$. In particular, if $A > 1 - \eta$ and $B < \eta$, with $\eta \ll 1$ then $\delta(\eta) \sim \frac{1}{2}\sqrt{\eta}$.

Proof. Follows [16], Theorem 4, see also [30] where some slight variants were also proved. □

In what follows, we will consider a q-state spin system with the additive internal symmetry. The lowest energy is for complete alignment and the gap will be set to one: $\mathscr{E}_0 = -1$. In addition, there will be s non-zero-energy levels corresponding to $2s$ distinct alignments relative to the state 0: $-1 < \mathscr{E}_1 = \mathscr{E}(0, \alpha_1^{\pm}) \leqslant \mathscr{E}_2 = \mathscr{E}(0, \alpha_2^{\pm}) \leqslant \cdots \leqslant \mathscr{E}_s = \mathscr{E}(0, \alpha_s^{\pm}) < 0$. For large q, under the condition that s/q is small and that most of the energies are close to zero, it will be shown that there is a first-order transition directly into the magnetized phase. Here, in the graphical representation, one anticipates a discontinuous percolation transition from a state where occupied bonds of any type are rare into a state where most of the bonds are blue and belong to an infinite cluster. On the other hand, if either of the above-mentioned conditions are violated, there can be an intermediate phase corresponding to the percolation of various other colors. Since the problem with a single transition is easier both conceptually and analytically, let us begin with these cases.

Lemma 4.3. Consider a spin system/graphical problem with the above described symmetry at inverse temperature β on a diagonal torus with $N = 2^n$ sites and let $\mathbb{P}(-)$ denote the associated probability measure. Let $b = \langle i, j \rangle$ denote a given bond and let

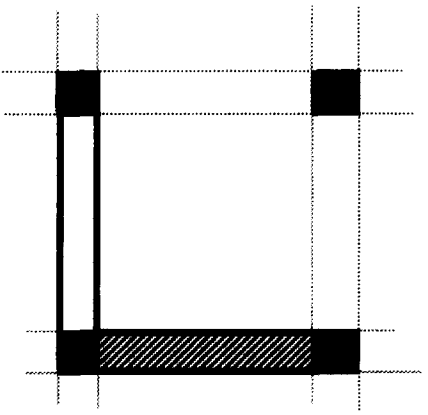

a: The event

Fig. 2.

b_0, $b_1^{\pm},\ldots b_k^{\pm}$ denote the event that this bond is occupied and is colored *blue*, $red_1^{\pm},\ldots,$ $red_s^{\pm}$ corresponding to the appropriate energy state and let $b_\emptyset$ denote the event that this bond is vacant. Then $\mathbb{P}(b_0)\leqslant q^{1/2N}R_0/[Z]^{1/2N}$, $\mathbb{P}(b_k^+)=\mathbb{P}(b_k^-)\leqslant q^{1/2N}R_k/[Z]^{1/2N}$, $k=1,\ldots,s$ and $\mathbb{P}(b_\emptyset)\leqslant q^{1/2}/[Z]^{1/2N}$ where Z denotes the partition function (i.e. the sum of all the graphical weights as written in Eq. (2.8)).

Proof. Consider, for example, the event b_0 that the bond $\langle i,j\rangle$ is blue. If ϑ' is the reflection through a line containing i, the Cauchy–Schwartz inequality reads $\mathbb{E}(b_0)\leqslant[\mathbb{E}(b_0\,\vartheta' b_0)]^{1/2}$. The square of the upper bound is the probability of two blue bonds sharing the endpoint i. Repeated reflections are performed, doubling the size of the cluster at each stage until the entire torus is covered, a total of $n+1$ times. The ultimate estimate is therefore the $1/(2N)$th root of the probability that all the bonds on the torus are blue. The latter has the interpretation of the ratio of the *constrained* partition function in which all bonds are blue, Z_0, to the total partition function Z. The calculation of Z_0 is trivial: if each blue bond is occupied, the fugacity factor is R_0^{2N} and are exactly q (fully ferromagnetic) spin configurations that are consistent with this bond configuration. The bounds on the other probabilities follow similarly. In the "all vacant" case, where the associated constrained partition function may be denoted as $Z_\emptyset$, the result $Z_\emptyset=q^N$ follows from the fact that every spin configuration is consistent with all bonds being vacant. □

The graphical picture of such a single transition is that, depending on the temperature, the dominant configuration is either all blue or all vacant and then at some temperature, both of these "states" are allowed. Thus, the first ingredient is the assertion that the probability of anything else, i.e. a red bond, is uniformly small. Then it must be shown that the simultaneous presence of vacants and blues is always unlikely. The

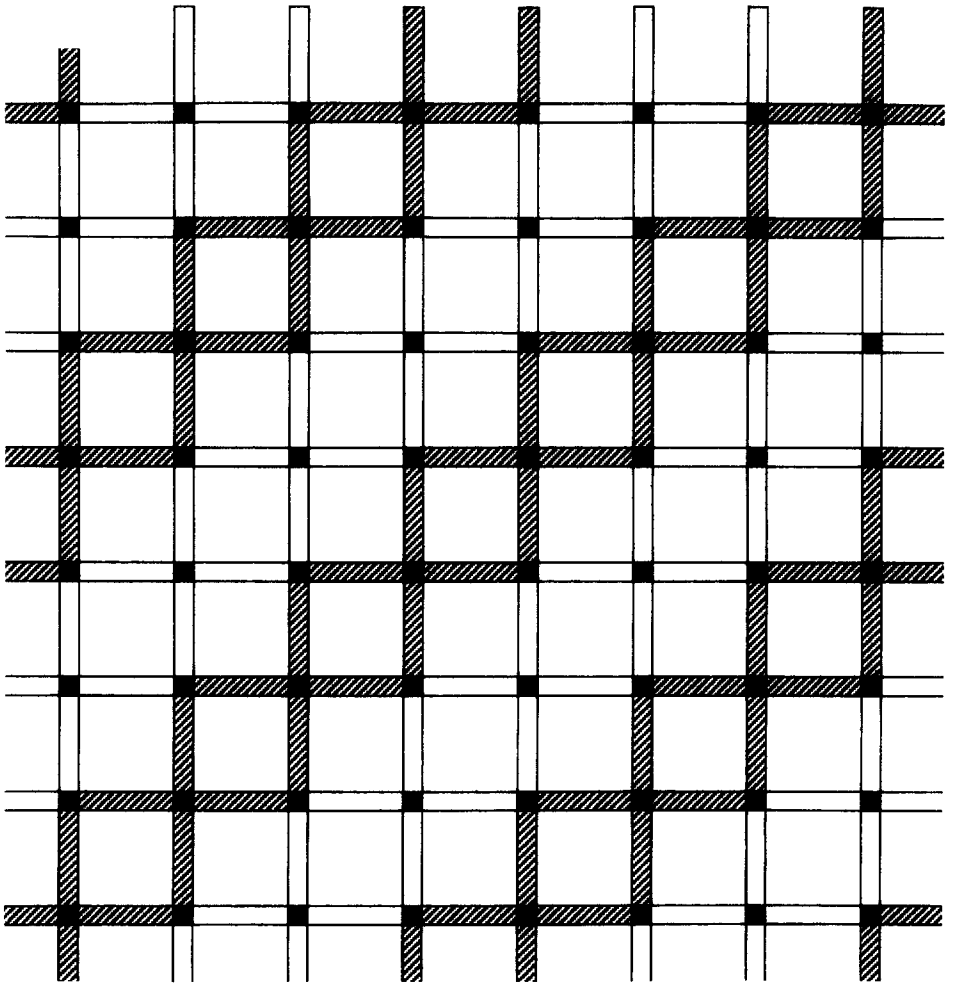

b: The pattern

Fig. 2. Continued.

second issue requires an additional RP derivation but the first can be handled on the basis of Lemma 5.3. Indeed, for all temperatures, the bounds

$$\mathbb{P}(b_k) \leqslant \frac{(\sqrt{q}+1)^{|\mathcal{C}_k|-1}}{\sqrt{q}} \equiv V_k \leqslant q^{-(1/2)[1-|\mathcal{C}_k|]} \tag{4.3}$$

are readily obtained. Starting with $Z \leqslant Z_\emptyset + Z_0$, we have

$$\mathbb{P}(b_k) \leqslant \frac{R_k}{[R_0^{2N} + q^N]^{1/2N}} \,. \tag{4.4}$$

For $q \geqslant R_0^2$, we may neglect the smaller term in the denominator and the resulting expression is increasing in β and hence should be evaluated at the temperature where $R_0 = q^{1/2}$. At this temperature, $R_k = (\sqrt{q}+1)^{|\ell_k|} - 1)$ which is in turn less than $q^{(1/2)\ell_k}$. On the other hand, for $R_0 \geqslant q^{1/2}$, we neglect the q^N in the denominator. It is readily demonstrated that R_k/R_0 is decreasing in β hence this estimate is maximized at the point where $R_0 = q^{1/2}$ as well.

As an indication that coexistence is unlikely, let us start with the (necessary) demonstration that the probability of a vacant and blue bond sharing an endpoint is uniformly small:

Lemma 4.4. Let $i \in \mathscr{T}_N$, and let $b = \langle i, j\rangle$ with $j - i = (1,0)$ and $b' = \langle i, j'\rangle$ with $j' - i = (0,1)$ denote a pair of adjacent bonds. Then, for a system as described in Lemma 4.3,

$$\mathbb{P}(b_0 \cap b'_\emptyset) \leqslant q^{-1/4}$$

Proof. The event, as depicted in Fig. 2(a) after n reflections results in the pattern depicted in Fig. 2(b). Let us denote the associated partition function by $Z_{0\emptyset}$. As $N \to \infty$, the only important features are that $Z_{0\emptyset}$ has half the bonds blue, the other half vacant and one quarter of the sites unconstrained. Thus we may write $Z_{0\emptyset} = q^{(1/4)N} R_0^N \Phi_N$ with $[\Phi_N]^{1/N} \to 1$ as N tends to infinity. Estimating $Z \geqslant Z_0 + Z_\emptyset$, we obtain

$$\mathbb{P}(b_0 \cap b_\emptyset) \leqslant \frac{q^{1/4} R_0}{[q^N + R_0^{2N}]^{1/N}} \Phi_N^{1/N} . \tag{4.5}$$

The right-hand side is optimized when $R_0^2 = q$ resulting in the stated bound. □

The final ingredient that we will need is a contour estimate. If $\ell \in \mathscr{T}_N$, let $b_0(\ell)$ denote the event b_0 translated to the bond $\langle i + \ell, j + \ell\rangle$ and similarly for the events $b_s^+(m)$, etc. Let us consider the simultaneous occurrence of the events $b_0(\ell)$ and $b_\emptyset(m)$. In a given configuration, let us call any site in which the four bonds that emanate from it are all vacant or all blue a *good* site. Any other site will be deemed to be a *contour* site. It is clear that if the events $b_0(\ell)$ and $b_\emptyset(m)$ both occur, than any connected path from one of the blue endpoints (at $i + \ell$ or $j + \ell$) to one of the vacant endpoints (at $i + m$ or $j + m$) must use at least one contour site. This implies that the respective bonds are separated by a $*$-connected circuit of contour sites which leads to:

Lemma 4.5. Let ε $(= \varepsilon(\mathscr{H}))$ denote the quantity $5q^{-1/4} + 8\sum_k V_k$. Then, for ε sufficiently small,

$$\mathbb{P}(b_0(\ell) \cap b_\emptyset(m)) \leqslant c_1 \varepsilon$$

with c_1 a constant of order unity holds for all $\ell, m \in \mathscr{T}_N$.

Proof. As mentioned previously, the bonds in question are separated by a $*$-connected circuit of contour sites, a contour. For a given contour, C, of length $|C|$, the standard

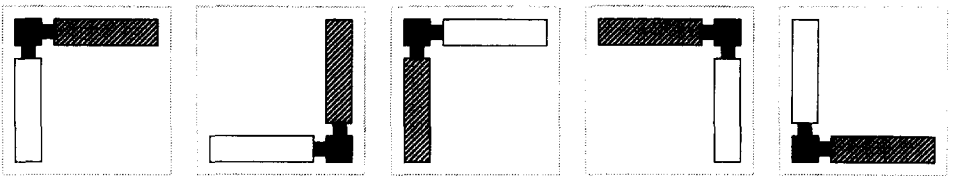

Fig. 3.

chessboard estimate allows us to break the contour into its constituents and apply the previous estimates to each piece. Provided that all quantities are sufficiently small, this will result in an estimate on $\mathbb{P}(C)$ that is exponentially small in $|C|$.

Since the events in question actually involve bonds, let us conservatively select only one in five sites of C to insure that we do not count any bond twice. (More precisely, we use $[\frac{1}{5}|C|]^+$ sites where $[-]^+$ denotes "smallest integer larger than".)

For contour sites that are endpoints of red bonds, there are a total of two species of each color and four lattice orientations, which accounts for the factor of eight in front of the sum of the V_k's. If a site houses both vacant and blue bonds, then, as is easily checked, one of the five configurations depicted in Fig. 3 must occur. Hence the factor of five in front of the $q^{-1/4}$.

Performing a standard Peierls estimate, where the minimal contour size is two, the stated result follows if ε is sufficiently small. □

Theorem 4.6. Consider a q-state spin system as described in Eqs. (2.1)–(2.4) with $\varepsilon = \varepsilon(\mathscr{H})$ as described in Lemma 4.5 sufficiently small. Then there is an inverse temperature β_t at which there exists (at least) $q+1$ distinct phases. One of these is a high-temperature phase characterized by the exponential decay of the two-point correlation function and the other q are the various magnetized phases. In the graphical representation, the magnetized phases correspond to a phase with an infinite cluster of blue bonds while in the disordered state, the cluster connectivity decays exponentially. Hence, this system exhibits a discontinuous percolation transition in the grey and in the multicolored representation.

Proof. The existence of a transition temperature $1/\beta_t$ where high- and low-temperature phases coexist is a direct consequence of Lemma 4.2 and the estimates obtained in Lemmas 4.3–4.5.

In what follows, it would be convenient to assert that the high- and low-temperature phases actually emerge, in the form of a convex combination, simply by taking the thermodynamic limit of the torus states. However, such an assertion can only be proved in special cases [32]. We may circumvent this minor difficulty by adding to the Hamiltonian a local term that couples linearly to the desired bond event. For example, in the case of blue bonds, we fix all parameters save for the lowest energy level which

we now write as $\mathscr{E}_0(1+\lambda)$.[5] Then, for a discussion of the low-temperature phase we may consider the $\lambda \downarrow 0$ limit of the positive λ states that are limits of states on $\mathscr{T}_N$. By the usual convexity arguments, any $\lambda = 0^+$ state cannot have a smaller blue bond density than any state constructed from the $\lambda = 0$ Hamiltonian. It is further noted that the estimates obtained in Lemmas 4.2–4.5 are continuous in all parameters and hence may be freely used for $|\lambda| \ll 1$. It follows that we can find a sequence $N_j \to \infty$ and $\lambda_j \to 0$ such that in the finite volume states $\mathbb{P}_{N_j,\beta_t,\lambda_j}(-)$ the results of the above mentioned hold and we may rest assured that for all j, $\mathbb{P}_{N_j,\beta_t,\lambda_j}(b_0) \geqslant 1-\delta$. Similar devices will be used in our discussion of other states.

Let us start with a proof that at β_t there is a percolating state in the graphical representation. Consider a box of side k lying in the center of a box of side $L(N) \gg k$ with $L \to \infty$ as $N \to \infty$. Let B_k denote the event that there is a connection between the two boxes by a path of "good" sites. It is clear that the event B_k occurs with probability close to one because the complementary event requires that a contour surround the inner box:

$$\mathbb{P}_{N_j,\beta_t,\lambda_j}(B_k) \geqslant 1 - c_2' \varepsilon^{c_2 k} \tag{4.6}$$

where the c_2's are constants of order unity and ε is now taking on some mild λ dependence.

Notice that B_k may be written as the disjoint union of two events depending on what type of good sites are making the connection: $B_k = B_k^{\emptyset} \cup B_k^0$. We claim that if k is large enough, $\mathbb{P}_{N_j,\beta_t,\lambda_j}(B_k^0)$ is bounded below uniformly in j. Indeed, for any bond b that is well separated from the boxes,

$$1 - \delta \leqslant \mathbb{P}_{N_j,\beta_t,\lambda_j}(b_0 \cap B_k^0) + \mathbb{P}_{N_j,\beta_t,\lambda_j}(b_0 \cap B_k^{\emptyset}) + \mathbb{P}_{N_j,\beta_t,\lambda_j}(b_0 \cap \tilde{B}_k) \tag{4.7}$$

where the tilde denotes complementation. The third term may be estimated by $c_2' \varepsilon^{c_2 k}$ and the first by $\mathbb{P}_{N_j,\beta_t,\lambda_j}(B_k^0)$. As for the second term, it is clear that the event $b_0 \cap B_k^{\emptyset}$ implies that there is a contour surrounding b (or, negligibly unlikely in the large j limit, a counter surrounding the good sites that caused the event B_k). This can be handled by the techniques of Proposition 4.5. Hence $\mathbb{P}_{N_j,\beta_t,\lambda_j}(B_k^0) \geqslant 1 - \delta - \frac{1}{2} c_1' \varepsilon - c_2' \varepsilon^{c_2 k}$ (with c_1' essentially the same as c_1 from Proposition 4.5) and we have established the percolation claim.

Let us now turn attention to connectivity function in a "vacant" state. Let κ be the parameter that couples linearly to the vacant bond density and consider the torus states $\mathbb{P}_{N_j,\beta_t,\kappa_j}(-)$ that are tending to a limiting state with bond density less than δ. Further, consider the event $\bar{B}_k^{\emptyset}$ that is the event $B_k^{\emptyset}$ translated to the back of the torus. By an argument similar to that used above, $\mathbb{P}_{N_j,\beta_t,\kappa_j}(\bar{B}_k^{\emptyset})$ is uniformly positive and hence any limit of the conditional measures $\mathbb{P}_{N_j,\beta_t,\kappa_j}(- \mid \bar{B}_k^{\emptyset})$ is also a state with low bond density. Now let i and i' be two (fixed) sites and consider the event $T_{i,i'}$ that these sites belong to the same cluster of occupied bonds. The event $\bar{B}_k^{\emptyset} \cap T_{i,i'}$ implies the existence of

[5] It is obvious from the Edwards–Sokal form of the weights that the derivative of the (finite volume) free energy with respect to λ is proportional to the blue bond density.

a contour surrounding i and i' (or the box in which $\bar{B}_k^{\emptyset}$ occurs) and hence may be estimated by

$$\mathbb{P}_{N_j,\beta_t,\kappa_j}(T_{i,i'} \mid \bar{B}_k^{\emptyset}) \leqslant c_3' \varepsilon^{c_3|i-i'|} \tag{4.8}$$

where the c_3's are further constants of order unity. Clearly, the exponential decay of the cluster connectivity function implies the exponential decay of the two point function.

Finally, using a similar sort of conditioning at the back of the torus and, in the spin system further conditioning on the spin-state of the largest cluster, it is straightforward to show that the spin-marginals of $\mathbb{P}_{N_j,\beta_t,\lambda_j}$ converge to magnetized states of which there are a total of q. □

In [18], it was established that for large q, the q-state Potts models did, after all have a phase transition at the self-dual point. The above provides a simpler argument:

Corollary. Consider the usual q-state Potts models on $\mathbb{Z}^2$. Let β denote the inverse temperature and, as usual, $p = 1 - e^{-\beta}$. Then for all q sufficiently large, there is a single ordering transition at β_c given by $p_c = p(\beta_c) = \sqrt{q}/[1 + \sqrt{q}]$. In particular, at β_c, there are (at least) $q+1$ phases coexisting. For all $\beta < \beta_c$, there is a unique phase characterized by exponential decay of correlations. For all $\beta \neq \beta_c$, the energy density is continuous and for all $\beta > \beta_c$, the magnetization is continuous.

Proof. Suppose that q is large enough that all the preceding applies. Let β_t denote "any" point where there are co-existing phases with bond densities above $1 - \delta$ and below δ. By convexity and monotonicity, it follows that β_t is unique: if $\beta > \beta_t$, then in any state, the bond density is greater than $1-\delta$ and if $\beta < \beta_t$ it is less than δ. Similarly, it follows that if for some value of β, the bond density in any regular sequence of volumes is bounded away from δ and $1 - \delta$, then $\beta = \beta_t$. But when $p = p_c$, the bond density equals the vacant bond density on the torus because here, not only do the parameters transform into one another, so do the boundary conditions. Thus a phase transition occurs at p_c.

We claim that for $\beta < \beta_c$, the correlation length is positive, the magnetization is zero and the state is unique. Indeed, at $\beta = \beta_c$, by the arguments used in Theorem 4.6, there is a state that has exponential decay of the cluster connectivity function. Here, by the FKG property, it is not hard to see that this may be identified with the state arising from free boundary conditions. Now in general the bond density (or the energy density, cf. [8] Eq. (2.6)) as defined via a thermodynamic derivative is monotone and hence can have discontinuous at only a countable number of points. Furthermore, the range of allowed values that the bond density can take on at any particular value of β, is precisely the left and right limits of the (thermodynamic) density. Thus, at a point of continuity, only one value of the density is possible. Now, ostensibly at any $p(\beta)$, we have $\mu_{q,p}^{FK;w}(-) \geqslant_{\mathrm{FKG}} \mu_{q,p}^{FK;f}(-)$. However (cf. [33, Corollary 2.8]) if the densities coincide, so do the measures. Thus let $\beta < \beta_c$ be a point of continuity of the bond density. Obviously the free measure at β_c dominates the free measure at β and hence

$\mu^{FK;f}_{q,p(\beta)}(-)$ has exponential decay of the cluster connectivity. However, it was agreed that $\mu^{FK;f}_{q,p(\beta)}(-) = \mu^{FK;w}_{q,p(\beta)}(-)$ and hence there is also exponential decay in the wired state. This precludes percolation; hence the magnetization vanishes and there is uniqueness of the Gibbs state. Once this is established at β, it is automatically valid for any $\beta' < \beta$, and we can find points of continuity right up to β_c. Finally, suppose that $\beta > \beta_c$ and recall the construction of the magnetization order parameter in Theorem 3.3. In the present circumstances, once $\beta > \beta_c$, we have exponential decay of the dual connectivity function – long chains of dual bonds are exponentially improbable in their length. It follows that the magnetization can be uniformly approximated by finite events in finite boxes, e.g. the probability in a wired box of scale L_1 that the origin is connected to a cluster of scale at least as large as L_2 with $L_1 \gg L_2$ and L_2 large compared to the correlation length at β_c. Continuity of the magnetization is immediate. □

For particular models (in addition to the Potts models) the results of Theorem 4.6 may be improved by exploiting specialized features. Combining the large q arguments with the graphical representations for the generalized AT models, we have

Theorem 4.7a. Consider the generalized r,s-valued AT (cubic) models in the region $\Delta \leqslant 1$ parameterized by U and V as in Eq. (3.6b) or Eq. (3.10). Suppose that $q = rs$ is sufficiently large and let us move along a curve of constant V with $Vs^{-1/2}$ sufficiently large. Then there is a first-order transition at a value U_t given, approximately by $U_t \approx \sqrt{q}/V$. At $U = U_t$, there are (at least) $q+1$ coexisting phases one of which is high-temperature, e.g. has no magnetization and exponential decay of correlations and the others of which are low-temperature magnetized states. For $U > U_t$, there is a low-temperature magnetized phase and for $U < U_t$ there is a unique Gibbs state.

Proof. The estimates involving black and vacant bonds are identical to the blue and vacant estimates from Theorem 4.6 with R_0 replaced by UV. A black-vacant contour element is therefore uniformly small if $q^{1/4}$ is sufficiently large. Let b_w denote the event of a particular white bond. Then

$$\mu^{AT;\mathscr{T}_N}_{Q,P}(b_w) \leqslant \left[\frac{U^{2N}s^N}{(UV)^{2N} + r^N s^N}\right]^{1/2N} \leqslant s^{1/2}/V \tag{4.9}$$

where the left-hand side refers to the measure on the torus $\mathscr{T}_N$. By hypothesis, this is small and hence all the conditions of Lemma 4.5 are satisfied which implies the transition point conclusions, at some value U_t, of Theorem 4.6. If $U > U_t$, by FKG domination, we have "percolation" implying the existence of the low temperature phase. For $U < U_t$, we may assume, without loss of generality that U is a point of continuity of the *grey* bond density by an argument similar to that used in the corollary to Theorem 4.6. Then, as far as the grey measure is concerned, the state is unique and FKG dominated by the high-temperature state at the transition point. Uniqueness of the Gibbs state and exponential decay of correlations now follow easily. □

Theorem 4.7b. Consider the generalized r,s-valued AT (cubic) models in the region $2 \geqslant \Delta \geqslant 1$ parameterized by L, D and G as in Eq. (B.5). Consider a curve of fixed G and D with $0 \leqslant L \leqslant \infty$. Suppose that $q = rs$ is sufficiently large while $Gs^{-1/2}$ and $Dr^{-1/2}$ are sufficiently small. Then there is an L_t at which there is phase coexistence of q ordered and one disordered states (among possible others). For $L > L_t$ there is a low temperature magnetized phase and for $L < L_t$ there is a unique high-temperature state.

Proof. The disordered bonds are as before and will be estimated using the empty partition function $Z_\emptyset = q^N$. Here we define ordered as the presence of a double bond or the presence of a bond in both the top and bottom layers. The relevant partition function is $Z_0 = [L(1+G)(1+D) + GD]^{2N}$. The basic contour element, a site with at least one bond of each type, leads to the same estimate as the Potts model: $[Z_{0\emptyset}/Z]^{1/N} \leqslant q^{-1/4}$. The new ingredients are a bond in the top layer and a vacancy in the bottom layer and vice versa. The relevant estimates for these probabilities are $[G^{2N} r^N / Z] \leqslant Gs^{-1/2}$ and $[D^{2N} s^N / Z] \leqslant Dr^{-1/2}$. If all these quantities are sufficiently small, the stated result follows from arguments similar to the previous ones. □

Corollary. For the AT models described in Theorem 4.7a, on $\mathbb{Z}^2$ with $r = s = \sqrt{q}$ and all quantities sufficiently large or small as stated, the ordering transition occurs at $UV = \sqrt{q}$ (i.e. on the self-dual line found in Proposition B.1). For the models described in Theorem 4.7b, with $G/\sqrt{s} = D/\sqrt{r}$, and all quantities sufficiently large or small as stated, the ordering transition occurs at $L = [rs - rG^2]/[(1+G)(\sqrt{rs} + rG)]$.

Proof. In the reformed region, under the stated hypotheses, the white (and hence *white) bond densities are uniformly small as U is varied. The black and vacant densities are always small or close to one and hence never equal except as a consequence of phase coexistence at the transition point. But on the torus, these densities *are* equal when $UV = \sqrt{q}$ which identifies the critical point in this case.

In the orthodox region, under the stated hypotheses, the probability of only a κ-layer bond or only a τ-layer bond is uniformly small. Similarly, the probability of both, without the presence of a double bond, is estimated by $GD/\sqrt{rs}$ which is (doubly) small. Hence, the transition is signaled by an abrupt change in the density of double bonds (which is monotone in L) from small to large. Now the absence of a double bond on the dual lattice implies the presence of the corresponding ordinary double bond or the separate occurrence of single bonds in the top and bottom layer. Thus the double bond density and the dual bond density add up to nearly one. If they are equal – which occurs on the torus when L crosses the self-dual line, we have identified the transition point. □

Finally, we turn attention to the existence of intermediate phases. Starting with the usual sort of discrete spin system, we will show, under suitable hypotheses, that there is a discontinuous percolation transition in which the blue bonds play no essential role. We do not at present have a general proof that the magnetization vanishes in this phase

but we consider this to be highly plausible. Notwithstanding, we also suspect (again, by and large, without any rigorous proofs) that anything else is possible including phases characterized by a partial breakdown of symmetry, phases with a unique state characterized by exponential decay of correlations, and, in two dimensions, Berezinski–Kosterlitz–Thouless phases. In the former case, we will provide several examples, some of which include a proof that the magnetization actually vanishes. In all cases, there is a genuine low-temperature phase. One does not expect that the phase transition into this state will always be first order. However, under some added assumptions, we will show that this is sometimes the case.

The ingredient that is necessary for all of these arguments is a lower estimate on the graphically constrained partition function that is characteristic of the intermediate phase. The following, although far from optimal, will suffice for present purposes:

Proposition 4.8. Consider a discrete spin system of the type described and let Z_I denote the partition function on $\mathcal{T}_N$ corresponding to the graphical configurations in which all bonds of the torus are occupied by a non-blue bond. Then

$$Z_I \geqslant \left[\prod_{k>0} R_k^4\right]^{N/2} .$$

Proof. Let us consider only the configurations where all the spins on the even sublattice take on one fixed value. Now allow the spins on the odd sublattice to take on any of the s choices that are different from this fixed value and have negative pairing energy relative to this state. Connecting all spins with the appropriate colored bonds we get a covering of the torus by red crosses (reminiscent of Fig. 2(b)) each of which represents $2s$ independent choices with weights $R_1^4, \ldots, R_s^4$. The number of these crosses is $N/2$ and the stated estimate follows.

The following provides sufficient conditions for the existence of a "red" phase:

Theorem 4.9. Consider a discrete spin system of the type described and let $\tilde{\beta}_*$ denote the temperature at which

$$\left[2\sum_{k=1}^{s} R_k^4\right]^{1/2} = q .$$

Define $\kappa(q)$ by

$$\kappa(q) = \frac{1}{q^{3/4}}\left[R_0 + 2\sum_{k=1}^{s} R_k\right]_{\beta=\beta_*}$$

Suppose that there is a temperature $\tilde{\beta} < \tilde{\beta}_*$ at which

$$\frac{R_0}{[2\sum_{k=1}^{s} R_k^4]^{1/4}} < \varepsilon ,$$

that

$$\frac{q^{1/2}}{[2\sum_{k=1}^{s} R_k^4]^{1/4}} < \varepsilon$$

and that $\kappa(q) < \varepsilon$ for ε sufficiently small. Then there is a β_* at which two phases coexist exist. One of these is a identifiable as a high-temperature phase but the second is of indeterminate character. However, if $\langle i,j\rangle$ is a nearest-neighbor pair then for some k's, the probability that $\sigma_j = \sigma_i + \alpha_k$ is larger in the second state.

Remarks. If s is fixed and $q \to \infty$, the condition on $\kappa(q)$ will be satisfied for q large enough. The worst case is when all the R's are equal and here, $\kappa(q) \sim s^{3/4}/q^{1/4}$ When the degeneracy is this large, our estimates are rather inefficient and it is worthwhile to pay attention to the specifics of the model at hand. On the other hand, if there are just a few dominant energies, we get estimates similar to the Potts case even if s is comparable to q. Next, it is noted that if the low-energy states correspond to a subgroup of the spin-space, there is a genuine order parameter for the intermediate phase. The (r,s) models in the reformed region are a degenerate example of this situation. Finally, in all cases, it is a near certainty that under the conditions in the statement of Theorem 4.9, the energy itself is discontinuous at the transition temperature. However, the energy corresponds to a *weighted* sum of the described probabilities which might (miraculously) match in the two states. Needless to say, if the smallest energy gap times the bond density in the "red" state is large compared to the bond density in the high-temperature state, it is trivial to demonstrate that there is a jump in the energy.

Proof. The stated conditions easily allow us to verify what is required for Lemma 4.2 from which all the conclusions follow. The probability of a blue bond is estimated:

$$\mathbb{P}(b_0) \leqslant \frac{R_0^2}{[2\sum_k R_k^4]^{1/2}} \tag{4.10}$$

which, we claim, is an increasing function of β. Indeed, taking logarithmic derivatives, it is sufficient to show

$$|\mathscr{E}_0|\left(1 - \frac{1}{R_0}\right) \geqslant \overline{|\mathscr{E}_k|\left(1 - \frac{1}{R_k}\right)} \tag{4.11}$$

where the overbar denotes averaging with respect to the weights R_k^4. However, Eq. (4.11) holds for all k without averaging. This allows us to evaluate the right-hand side of Eq. (4.10) at $\beta = \tilde{\beta}$, where we get ε and the estimate holds for all β in $[\tilde{\beta}, \infty)$. There are no other possibilities for bonds except for red and vacant. The probability of a red bond and a vacant bond sharing a site is estimated by

$$\mathbb{P}(\langle i,j\rangle \text{ is red and } \langle i,j'\rangle \text{ is vacant}) \leqslant \frac{q^{1/4} 2\sum_{k>0} R_k}{[q^N + [2\sum_k R_k^4]]^{1/N}} \leqslant \kappa(q) \tag{4.12}$$

by evaluating at $\beta = \tilde{\beta}_*$. Thus, reds dominate at $\beta = \tilde{\beta}$, the vacants as $\beta \to \infty$, the blue bonds and the other contour elements are uniformly small for all $\beta \leqslant \tilde{\beta}$. The conclusions follow if ε is sufficiently small. □

As discussed earlier, additional assumptions are required to demonstrate a discontinuous transition into the low-temperature phase. Although this is obvious from a physical perspective, it is interesting to see how these considerations enter into our analysis. Here we see that the estimate on the constrained partition function for a red/blue contour element is the square root of the product of the separate partition functions. Hence, at the approximate transition temperature, the ratio is of order unity. Needless to say, if pertinent specifics are brought into play, better estimates may be obtained. For example, if there are g spin states with $g \gg 1$ such that the energy between any pair of these states is always lower than some $\mathscr{E}_g \gtrsim -1$ $(= \mathscr{E}_0)$, there will be a first-order transition into the blue phase. (The proof of this follows almost identically the proof for the Potts model and will be omitted.) For present purposes, we will be content with some results along these lines for the (r,s)-generalized AT models.

Theorem 4.10. Consider the (r,s)-generalized AT models in the region $\Delta < 1$ parameterized by U and V as in Theorem 4.7a first moving along a trajectory of constant V. Then for $V/s^{1/2}$ sufficiently small and r sufficiently large, there is a first-order transition into the intermediate phase at some $U_t = U_t(V)$. At $U = U_t$, at least $r+1$ phases coexist. Next, consider a trajectory of constant U with $U/r^{1/2}$ large. Then if s is sufficiently large, there is a first-order transition into the low-temperature phase at some $V_t(U)$ where at least $r+q$ phases coexist. As a consequence, if both r and s are sufficiently large, the upper and lower phase boundaries of the intermediate phase are lines of first-order transitions for all Δ sufficiently small.

Proof. For the first case, the probability of a black bond is estimated by $UV/[q^N + U^{2N}s^N]$. This never exceeds $Vs^{-1/2}$ which is assumed to be small. The estimate for the vacant-white contour element is of the standard Potts-type yielding an upper bound of $r^{-1/4}$. The conclusions concerning the entrance into this phase are now readily established.

Next, suppose we allow V to vary with U fixed so that $U/r^{1/2}$ is large. The probability of a vacant bond is estimated: $\mathbb{P}(b_\emptyset) \leqslant [[q^N]/[U^{2N}s^N]]^{1/2N} = r^{1/2}/U$ and is therefore uniformly small. The transition from the nearly all white (intermediate) phase to the nearly all black (magnetized) phase is essentially that of the s-state Potts model. In particular, the probability of the black–white contour element is bounded by $s^{-1/4}$. Thus, under the stated conditions, the entrance into the low-temperature phase is discontinuous.

As for the last claim, let us first consider the lines of constant U. These correspond to straight lines emanating from the zero temperature point on the Potts line $(\Delta = 0)$ hitting the degenerate line $(\Delta = 1)$ at a temperature that lowers with increasing U. Now $V_t(U)$ is decreasing with increasing U but the $U \to \infty$ limit of $V_t(U)$ is finite.

It then follows that the larger U transitions correspond to decreasingly smaller values of Δ and thus, if s is large enough, our results concerning the low-temperature phase transition hold for all Δ sufficiently small. Similarly, if V is held fixed and, e.g. satisfies $V \leqslant 1$, the value $U_t(V)$ is uniformly bounded away from zero and infinity. Hence, as is easily discerned, so is the transition temperature. However, as $V \to 0$, the lines of constant V are, asymptotically, of the form $\Delta \approx V\beta[1 - e^{-\beta}]$. Hence, the smaller V transitions correspond to decreasingly smaller values of Δ. Hence, under the stated hypotheses, our results concerning the upper phase boundary hold for all Δ sufficiently small. Evidently, if both r and s are large enough, both phase transitions are first-order for all Δ sufficiently small. □

Appendix A

A.1. Li–Sokal bounds

The Li–Sokal bound, in the case of the SW algorithm, is a direct consequence of a few facts about the algorithm all of which have been preserved in the above-described generalizations. What follows may appear to be "overly formal" however we would like to cover all the cases discussed in the remark preceding Lemma 2.1 as well as some further developments in the subsequent section. The specialized cases (pair interactions *and* no internal constraints on the allowed bonds within a single cluster) can be reduced from the derivation below or generalized from the original derivation in [5] with roughly the same amount of effort.

The "key inequality" leading to a Li–Sokal bound, (Eq. (1.1)) is that for some function Φ, the normalized autocorrelation function at unit time lag, $\rho_{\Phi\Phi}(1)$, satisfies

$$\rho_{\Phi\Phi}(1) \geqslant 1 - \frac{\text{const.}}{C_H} . \tag{A.1}$$

We will derive this on the basis of a few general features of the algorithms following closely the original derivation.

Starting (and staying) in some finite lattice Λ, a configuration, ω of the graphical representation is an assignment of zero or one: $\omega = (\omega_A \in \{0,1\} \mid A \in \mathscr{A})$ to each set A belonging to some distinguished collection $\mathscr{A}$ of ordered subsets of the lattice Λ e.g. ordered pairs of sites (bonds with possible repeats – "colors"). The sentence $\omega_A = 1$ or $\omega_A = 0$ signifies the presence or absence of the graphical element in a realization of the representation. A spin configuration $\underline{\sigma}$ is, as usual an assignment of a spin-value in $\{1,\ldots,q\}$ to each site of the lattice. To each ω_A, there is a number $p_A \in (0,1)$ that may be identified with the a priori probability of ω_A.

The presence of a graphical element on A implies that the spin configuration on A, denoted by σ_A must be in a restricted class of spin configurations, denoted by Σ_A. We will abuse notation and let Σ_A also denote the full class of configurations (on $\{1,\ldots,q\}^\Lambda$) with this configuration on A. It may be the case that for various $B \in \mathscr{A}$,

that have sites in common with A, the presence of ω_A forces the absence of ω_B, i.e. (exploiting the abusive notation) $\Sigma_B \cap \Sigma_A = \emptyset$. Any two such elements are called *inconsistent*. A configuration ω is said to be consistent if the totality of all of its elements are consistent in this sense:

For $\mathbf{P} = (p_A \mid A \in \mathscr{A})$ let $B_P(\omega)$ denote the product:

$$B_{\mathbf{P}}(\omega) = \prod_{A:\omega_A = 1} p_A \prod_{B:\omega_B = 0} (1 - p_B) . \tag{A.3}$$

It is clear that the algorithm defined by (a) and (b) simulates the Edwards–Sokal joint measure with weights

$$W_{ES} = \Delta(\sigma, \omega) B_{\mathbf{P}}(\omega) \tag{A.4}$$

where $\Delta(\sigma, \omega)$ is one if σ and ω are compatible and zero otherwise. An application of (a) and (b) in succession is considered to be a single Monte Carlo step. Note that the algorithm is "ergodic" in the sense that any bond-spin configuration can be reached from any other, in one step, because each p_A is *strictly* less than one. (Constrained systems, with some of the p_A's equal to one can be treated in the same fashion but there is no guarantee of ergodicity and will not be discussed further.) Further, it is noted that the spin-moves themselves may require considerable computational effort, none of which has been factored into the forthcoming bounds.

The connection with an actual spin system follows the usual course:

Proposition A.1. Consider the Hamiltonian, defined for spin configurations on Λ, given by

$$\mathscr{H} = - \sum_{A \in \mathscr{A}} |\mathscr{E}_A| \chi(\sigma_A \in \Sigma_A)$$

(with each $\mathscr{E}_A < 0$) where $\chi(-)$ is one if the condition in the parentheses is satisfied and zero otherwise. Then the generalized SW algorithm defined by (a) and (b) simulates the Gibbs distribution of this Hamiltonian at inverse temperature β provided that

$$p_A = 1 - e^{-\beta |\mathscr{E}_A|}$$

Proof. For a spin configuration $\underline{\sigma}$, on Λ, let $\mathscr{A}_{\underline{\sigma}} \subset \mathscr{A}$ denote the set of all A's such that $\omega_A = 1$ is consistent with $\underline{\sigma}$. Explicitly, $A \in \mathscr{A}_{\underline{\sigma}}$ implies that $\underline{\sigma} \in \Sigma(\omega_A)$. The energy of $\underline{\sigma}$ is then just

$$\mathscr{H}(\underline{\sigma}) = - \sum_{A \in \mathscr{A}_{\underline{\sigma}}} |\mathscr{E}_A| \tag{A.5}$$

and the Gibbsian weight for $\underline{\sigma}$ is given by

$$\exp\{-\beta \mathscr{H}(\underline{\sigma})\} = \prod_{A \in \mathscr{A}_{\underline{\sigma}}} e^{\beta |\mathscr{E}_A|} = \prod_{A \in \mathscr{A}_{\underline{\sigma}}} \frac{1}{(1 - p_A)} . \tag{A.6}$$

On the other hand, when we calculate the spin-marginal for the weights in Eq. (A.4), each disallowed element, $B \notin \mathscr{A}_{\underline{\sigma}}$ causes a factor of $1 - p_B$ whereas each $A \in \mathscr{A}_{\sigma_1}$ may be present or absent with probability p_A and $(1 - p_A)$ adding to one. Thus, the spin marginal assigns to $\underline{\sigma}$ the weight

$$W_{ES}(\underline{\sigma}) = \prod_{B \notin \mathscr{A}_{\underline{\sigma}}} (1 - p_B) = \text{const.} \prod_{A \in \mathscr{A}_{\underline{\sigma}}} \frac{1}{(1 - p_A)} . \qquad \square \tag{A.7}$$

We are ready for

Theorem A.2. Consider a generalized SW algorithm as defined by (a) and (b) above and let $\langle - \rangle$ denote the equilibrium measure for the process. Let $|\Lambda|$ denote the number of spins let $C_H = \beta^2[\langle \mathscr{H}^2 \rangle - \langle \mathscr{H} \rangle^2]/|\Lambda|$ be the heat capacity and let τ denote the integrated or exponential correlation time. Then τ obeys a Li–Sokal bound

$$\tau \geqslant [\text{const.}] C_H$$

where [const.] depends only on β and $\langle \mathscr{H} \rangle / |\Lambda|$ and hence, e.g. for systems with bounded and finite-ranged interactions, is uniformly bounded in the volume.

Remark. This result obviously covers all of the algorithms discussed in this section and in addition it covers all of the further developments in the subsequent section.

Proof. We will only derive the bound in Eq. (A.1). The connection between this and the stated bound, given the fact that in these algorithms we might as well have been applying a superfluous spin move on each Monte Carlo step, is made clear in [5]. For conceptual ease, let us assume that the bond moves take place at integer times: $t = 0, \pm 1$, etc. and the spin moves at half-odd integer times: $t = \pm \frac{1}{2}, \pm \frac{3}{2}$, etc. Our first claim is that

$$\langle \omega_A(t) \,|\, \underline{\sigma}(t \pm \tfrac{1}{2}) \rangle = p_A[\chi(\underline{\sigma}(t \pm \tfrac{1}{2}) \in \Sigma_A)] . \tag{A.8}$$

Indeed, for $\underline{\sigma}(t - \frac{1}{2})$ this follows directly from the algorithm. For $\underline{\sigma}(t + \frac{1}{2})$, the argument is apparently more difficult but the answer has to come out same as the one for $\underline{\sigma}(t - \frac{1}{2})$ because the joint distributions of $(\omega(t), \underline{\sigma}(t - \frac{1}{2}))$ and $(\omega(t), \underline{\sigma}(t + \frac{1}{2}))$ are given by the same weights, namely those in Eq. (A.4). (If the reader is dissatisfied with this overly smooth derivation, a calculation involving the ES weights, detailed balance and the connection with the graphical and Gibbsian weights may be performed directly. After a near miraculous cancellation, the stated result emerges.) Next, it is noted that given the spin configuration at time $t + \frac{1}{2}$, the graphical configurations at times t and $t + 1$ are independent so

$$\langle \omega_A(t) \omega_B(t + 1) \,|\, \underline{\sigma}(t + \tfrac{1}{2}) \rangle = p_A p_B[\chi(\underline{\sigma}(t + \tfrac{1}{2}) \in \Sigma_A \cap \Sigma_B)] . \tag{A.9}$$

At equal times, if $A \neq B$, we get the same formula for $\langle \omega_A(t)\omega_B(t) \,|\, \underline{\sigma}(t+\frac{1}{2})\rangle$ as in the right-hand side Eq. (A.9) however, if $A=B$ we reduce to the case calculated in Eq. (A.8). We define

$$\Phi(t) = \sum_{A \in \mathscr{A}} \frac{\mathscr{E}_A}{p_A} \omega_A(t) \tag{A.10}$$

so that

$$\langle \Phi(t+1)\Phi(t)\rangle = \sum_{A,B} \mathscr{E}_A \mathscr{E}_B \langle \chi(\underline{\sigma} \in \Sigma_A \cap \Sigma_B)\rangle = \langle \mathscr{H}^2 \rangle \,. \tag{A.11}$$

Meanwhile,

$$\langle \Phi^2(t)\rangle = \langle \mathscr{H}^2\rangle + \sum_A \mathscr{E}_A^2 \left(\frac{1}{p_A} - 1\right) \langle \chi(\underline{\sigma} \in \Sigma_A)\rangle \,. \tag{A.12}$$

For aesthetic purposes, we may bound the second term above by $\beta^{-1}|\langle \mathscr{H}\rangle|$. Thus,

$$\rho_{\Phi\Phi}(1) \equiv \frac{\langle \Phi(t+1)\Phi(t)\rangle - \langle \Phi\rangle^2}{\langle \Phi^2\rangle - \langle \Phi\rangle^2} \geqslant \frac{C_H}{C_H + \frac{\beta}{|\Lambda|}|\langle \mathscr{H}\rangle|} \tag{A.13}$$

which implies the stated claim. □

Appendix B

B.1. Duality on the square lattice

Duality on $\mathbb{Z}^2$ for the graphical representations of the cubic models is straightforward however different derivations are required for the two regions. Let us start with:

B.1.1. Duality in the reformed region

Consider the AT-random cluster models on the square lattice with parameters $P = (g,a)$ and $Q = (r,s)$. We may write the weights as in Eq. (3.6b):

$$W_{Q,P}{}^{AT}(\omega,\eta) = U^{N(\omega)} r^{c(\omega)} V^{N(\eta)} s^{c(\eta)} \chi_{\eta \subset \omega} \tag{B.1}$$

or, in "loop form"

$$W_{Q,P}{}^{AT}(\omega,\eta) \propto \left(\frac{U}{r}\right)^{N(\omega)} r^{\ell(\omega)} \left(\frac{U}{s}\right)^{N(\eta)} s^{\ell(\eta)} \chi_{\eta \subset \omega} \tag{B.2}$$

(as discussed in the proof of Proposition 3.5). Dual configurations are bond configurations on the dual lattice, $(\mathbb{Z}+\frac{1}{2})^2$, the dual of a *direct* bond is the edge traversal to it on $(\mathbb{Z}+\frac{1}{2})^2$. If ζ is a collection of direct bonds, let $\mathscr{D}(\zeta)$ denote the following set of dual bonds the elements of which be denoted by $*$'s: (1) black* bonds are dual to the vacant bonds (2) vacant bonds of the dual configuration are those dual to the

blacks of the direct configuration. (3) white and white* bonds are the duals of each other. This may be summarized by

$$\eta^* = \mathscr{D}(\omega^c), \qquad \omega^* = \mathscr{D}(\eta^c). \tag{B.3}$$

From Eq. (B.3) we have $N(\eta^*) = [\text{const.}] - N(\omega)$ and $N(\omega^*) = [\text{const.}] - N(\eta)$. Now, in general, each loop of direct bonds encircles a component of the dual configuration. Thus, save, perhaps for a constant, we get $c(\eta^*) = \ell(\omega)$ and $c(\omega^*) = \ell(\eta)$. Evidently,

$$W_{Q,P}{}^{AT}(\omega,\eta) \propto \left(\frac{s}{V}\right)^{N(\omega^*)} s^{c(\omega^*)} \left(\frac{r}{U}\right)^{N(\eta^*)} r^{c(\eta^*)} \chi_{\eta^* \subset \omega^*} \tag{B.4}$$

where, in the general case, the above must be properly interpreted in accord with the boundary conditions. It is amusing, as noted above, that for $r \neq s$, these models have been turned "inside out" under duality. In any case, Eq. (B.4) provides us with the simple duality relation $s^* = r$, $r^* = s$, $U^* = s/V$ $V^* = r/U$. A full statement and some consequences is as follows.

Proposition B.1. The generalized AT-models and/or the AT-random cluster models with parameters $(Q,P) = ((r,s),(g,a))$ are equivalent (i.e. dual to) the models with parameters (Q^*,P^*) given by

$$Q^* = (s,r),$$

$$g^* = \frac{sr(1-g) + sg(1-a)}{ag + sr(1-g) + sg(1-a)},$$

and

$$a^* = \frac{r(1-g)}{r(1-g) + g(1-a)}.$$

In case $r = s \equiv \sqrt{q}$, these models are self-dual along the curve given by

$$g = \frac{\sqrt{q}}{a + \sqrt{q}}.$$

Thus, if there is a single non-analyticity of the free energy as β is varied, it happens on this curve.

Proof. The formulas follow from the duality relations $U^*V = s$ and $V^*U = r$. Since, for $r = s$, the free energies at dual points are analytically related, if, as β is varied, there is a single phase transition (in the classic sense) it must occur along the self-dual line. □

Remark. Although the sentence concerning the single transition is surely vacuous for the usual AT model, if q is sufficiently large, we have shown that a phase transition indeed occurs along the $\Delta \lesssim 1$ portion of the self-dual line. It is tempting to conjecture that in general, the high- and low-temperature phase boundaries are images of one

another under the above duality. For $q=1$, this is easily verified: the high/low temperature phase boundaries are given by $g=p_c$ and $ag=p_c$ respectively with $p_c=\frac{1}{2}$. Here, the dual image of (a,g) is $(g^*,a^*)=(1-ag,[1-g]/[1-ag])$ so if $g=p_c$ then $a^*g^*=1-p_c=\frac{1}{2}=p_c$. For large q, some additional results on this matter can be derived. However, observe that for any q, the result follows asymptotically as $\Delta\to 0$ provided that one is prepared to accept that the transition temperature in the q-state Potts model is given by *its* self-dual point $p^*(q)=(\sqrt{q})/(1+\sqrt{q})$.[6] Indeed, in our limit $\beta\to\infty$, $\beta\Delta\to\alpha$ (which is controlled by the domination arguments) we have $g\to 1$ and $a\to 1-e^{-\alpha}\equiv a_\alpha$. The dual of these quantities satisfy $a^*\to 0$ and $g^*\to[\sqrt{q}(1-a_\alpha)]/[a_\alpha+\sqrt{q}(1-a_\alpha)]$, which, identifying $a=p$ and $g^*=p^*$ (as we should) is the usual duality for the $\sqrt{q}$–state Potts model.

B.1.2. Duality in the orthodox region

The duality relations in the orthodox region are slightly more involved. Let us start by writing the configurational weights in fugacity form:

$$Y^{AT}_{Q,P}\propto G^{N(\omega_\kappa)}D^{N(\omega_\tau)}L^{N(\omega_{\kappa\tau})}r^{c_\tau(\omega)}s^{c_\kappa(\omega)} \tag{B.5}$$

with $G=p_\kappa/[1-p_\kappa]$, etc. Now define $\Omega_\kappa=\omega_\kappa\vee\omega_{\kappa\tau}$ and $\Omega_\tau=\omega_\tau\vee\omega_{\kappa\tau}$ to be configurations for the κ and τ layers that count the presence of either a single or double bond. Note that $c_\kappa(\omega)=c(\Omega_\kappa)$ and similarly for $c_\tau(\omega)$. We claim that the weights can now be resummed into the form

$$X^{AT}_{Q,P}\propto \mathbf{A}^{N(\Omega_\kappa\vee\Omega_\tau)}\mathbf{B}^{N(\Omega_\kappa\wedge\Omega_\tau)}\mathbf{C}^{[N(\Omega_\kappa)-N(\Omega_\tau)]}r^{c(\Omega_\tau)}s^{c(\Omega_\kappa)}\,. \tag{B.6}$$

Indeed, the r and s factors are already in this form and the rest may be done bond by bond. For a given bond b, it is clear that $\omega_\kappa(b)=\omega_\tau(b)=\omega_{\kappa\tau}(b)=0$ if and only if $\Omega_\kappa(b)=\Omega_\tau(b)=0$ (and hence $\Omega_\kappa(b)\vee\Omega_\tau(b)=\Omega_\kappa(b)\wedge\Omega_\tau(b)=\Omega_\kappa(b)-\Omega_\tau(b)=0$) which serves to normalize the weights. Next, if $\omega_\kappa(b)=1$ while $\omega_\tau(b)=\omega_{\kappa\tau}(b)=0$ we have the unique contribution to the configuration where $\Omega_\kappa(b)=1$ and $\Omega_\tau(b)=0$ (and hence $\Omega_\kappa(b)\vee\Omega_\tau(b)=1$, $\Omega_\kappa(b)\wedge\Omega_\tau(b)=0$ and $\Omega_\kappa(b)-\Omega_\tau(b)=1$). Thus,

$$G=\mathbf{AC}\,. \tag{B.7a}$$

Similarly, if we consider $\omega_\tau(b)=1$ while $\omega_\kappa(b)=\omega_{\kappa\tau}(b)=0$, we arrive at

$$D=\mathbf{AC}^{-1}\,. \tag{B.7b}$$

All other configurations in the ω-system lead to $\Omega_\kappa(b)\vee\Omega_\tau(b)=\Omega_\kappa(b)\wedge\Omega_\tau(b)=1$ and $\Omega_\kappa(b)-\Omega_\tau(b)=0$ which implies

$$L(1+G)(1+D)+GD=\mathbf{AB}\,. \tag{B.7c}$$

Next, let us write Eq. (B.6) in loop form. Modulo unimportant constants, we have $c(\Omega_\kappa)=\ell(\Omega_\kappa)-N(\Omega_\kappa)$ and similarly for $c(\Omega_\tau)$. Now, we express $N(\Omega_\kappa)=\frac{1}{2}[N(\Omega_\kappa)+$

[6] This is, of course known, by rigorous standards, for $q=1$ and 2. For $q\gg 1$, even in the non-integer cases, this has been established by contour methods in [18]. The methods of Section 4 allow for a more direct proof.

$N(\Omega_\tau)] + \frac{1}{2}[N(\Omega_\kappa) - N(\Omega_\tau)]$ and do the same for $N(\Omega_\tau)$. Noting that $N(\Omega_\kappa) + N(\Omega_\tau) = N(\Omega_\kappa \vee \Omega_\tau) + N(\Omega_\kappa \wedge \Omega_\tau)$, we arrive at

$$X^{AT}_{Q,P}(\Omega) \propto \left[\frac{\mathbf{A}}{\sqrt{rs}}\right]^{N(\Omega_\kappa \vee \Omega_\tau)} \left[\frac{\mathbf{B}}{\sqrt{rs}}\right]^{N(\Omega_\kappa \wedge \Omega_\tau)} [\mathbf{C}\sqrt{r/s}]^{|N(\Omega_\kappa) - N(\Omega_\tau)|} r^{\ell(\Omega_\tau)} s^{\ell(\Omega_\kappa)} . \quad \text{(B.8)}$$

Now, consider the standard duality for the Ω-system, e.g. occupied Ω_κ bonds represent vacant Ω^*_κ bonds on the dual lattice, etc. It is clear that $\Omega_\kappa(b) \wedge \Omega_\tau(b) = 0 \Leftrightarrow \Omega^*_\kappa(b^*) \vee \Omega^*_\tau(b^*) = 1$ and similarly $\Omega_\kappa(b) \vee \Omega_\tau(b) = 1 \Leftrightarrow \Omega^*_\kappa(b^*) \wedge \Omega^*_\tau(b^*) = 0$ where b^* denotes the bond transverse to b. Furthermore, loops transform into components as usual, i.e. $\ell(\Omega_\kappa) \to c(\Omega^*_\kappa)$ and $\ell(\Omega_\tau) \to c(\Omega^*_\tau)$ and, finally, the $N(\Omega_\kappa) - N(\Omega_\tau)$ changes sign. Writing the dual weights in the form of Eq. (B.6), we get $\mathbf{B}^* = \sqrt{rs}\mathbf{A}^{-1}$, $\mathbf{A}^* = \sqrt{rs}\mathbf{B}^{-1}$ and $\mathbf{C}^* = \sqrt{s/r}\mathbf{C}^{-1}$. We transform this back into a formula for the weights in an ω-type system by inverting Eq. (3.7) and arrive at

$${}^*Y^{AT}_{Q,P} \propto [G^*]^{N(\omega^*_\kappa)} [D^*]^{N(\omega^*_\tau)} [L^*]^{N(\omega^*_{\kappa\tau})} r^{c_\tau(\omega^*)} s^{c_\kappa(\omega^*)} \quad \text{(B.9)}$$

with

$$G^* = \frac{sD}{L(1+G)(1+D) + GD} , \quad \text{(B.10a)}$$

$$D^* = \frac{rG}{L(1+D)(1+G) + DG} , \quad \text{(B.10b)}$$

and

$$L^* = \frac{rsL(1+G)(1+D)}{[L(1+G)(1+D) + G(r+D)][L(1+G)(1+D) + D(s+G)]} . \quad \text{(B.10c)}$$

The preceding derivation may be formalized:

Proposition B.2. Consider a generalized $Q = (s, r)$ AT-model with parameters $P = (p_\kappa, p_\tau, p_{\kappa\tau})$ so that the weight of a graphical configuration $\omega = (\omega_\kappa, \omega_\tau, \omega_{\kappa\tau})$ is given by

$$Y^{AT}_{Q,P}(\omega) = G^{N(\omega_\sigma)} D^{N(\omega_\tau)} L^{N(\omega_{\sigma\tau})} s^{c_\sigma(\omega)} r^{c_\tau(\omega)}$$

with $G = p_\kappa/(1 - p_\kappa)$, etc. Then, on $\mathbb{Z}^2$, this model is dual to the same model with parameters G^*, D^* and L^* as given in Eq. (B.10). In particular, this model is self-dual provided that $rG^2 = sD^2$ and, e.g. eliminating D,

$$L = \frac{rs - rG^2}{(1+G)(\sqrt{rs} + rG)} .$$

Proof. Follows from the above derivation. □

Remark. For r and s of order unity, there is not much that can be done to prove that the self-dual line is "the" transition line. However, for $r = 1$, the model is an effective s-state Potts model at inverse temperature β_{eff} given by $U_{eff} = e^{\beta_{eff}} - 1 = L + G + LG$.

Evaluating U_{eff} along the self-dual curve, we get $U_{eff}(L=L^*, D=D^*, L=L^*)=\sqrt{s}$ as expected. For various large values of the parameters r and s, it will be shown in the next section that the transition occurs at least on a portion of the self-dual curve.

B.2. An FKG property

Here we establish the result discussed after the statement of Proposition 3.2.

Lemma B.3. Consider a finite state space $\{A, B, \ldots, D\}$ with the order $A > B > \cdots > D$. Let Γ denote a finite set of points and suppose there is a measure $\mu_\Gamma(-)$ on $\{A, B, \ldots, D\}^\Gamma$ that assigns positive weight to each configuration and satisfies the lattice condition with respect to the associated partial order on the configurations. If $\alpha \in \{A, B, \ldots, D\}^\Gamma$ is a configuration, let $\zeta \in \{0,1\}^\Gamma$ be defined by $\zeta(i)=0$ if $\alpha(i)=D$ and $\zeta(i)=1$ otherwise. (The configurations ζ can therefore be thought of as equivalence classes of α's). Let ν_Γ be the measure on $\{0,1\}^\Gamma$ defined by

$$\nu_\Gamma(\zeta)=\sum_{\alpha\in\zeta}\mu_\Gamma(\alpha)\,.$$

Then $\nu_\Gamma(-)$ is strong FKG. Furthermore, if $\Xi \subset \Gamma$ and $* \in \{A, B, \ldots, D\}^\Xi$ is a "boundary condition" let $\nu^*_\Gamma(-)$ denote the "reduction" of this measure (which is itself FKG). Then if $*' \in \{A, B, \ldots, D\}^\Xi$ satisfies $*' \succ *$ we have

$$\nu^{*'}_\Xi(-) \underset{\text{FKG}}{\geqslant} \nu^*_\Xi(-)\,.$$

Proof. The fact that ν_Γ is FKG follows from the weaker statement that μ_Γ is FKG (as opposed to strong FKG). Indeed, let Φ and Ψ denote increasing events and define, e.g. $\tilde{\Psi} \in \{0,1\}^\Gamma$ by

$$\tilde{\Psi}=\{\alpha \mid \zeta(\alpha)\in\Psi\}\,. \tag{B.11}$$

It is obvious that $\tilde{\Psi}$ is increasing. Furthermore,

$$\nu_\Gamma(\Psi)=\sum_{\alpha\in\zeta}\mu_\Gamma(\alpha)\mathbb{1}_{\tilde{\Psi}}(\alpha)=\mu_\Gamma(\tilde{\Psi}) \tag{B.12}$$

where $\mathbb{1}_{\tilde{\Psi}}(-)$ is the indicator for $\tilde{\Psi}$. Hence $\nu_\Gamma(\Psi\cap\Phi)\geqslant\nu_\Gamma(\Psi)\nu_\Gamma(\Phi)$.

It also follows immediately that the various $\nu^*_\Xi(-)$ are FKG because if $\mu_\Gamma(-)$ is strong FKG then $\mu^*_\Xi(-)$ is FKG and the above applies. Suppose that $*' \succ *$. To establish that $\nu^{*'}_\Xi(-)\geqslant_{\text{FKG}}\nu^*_\Xi(-)$ it is sufficient to show that this is the case if we raise the value of $*$ at a single site. In turn, if $C' > C$ and $C(i)$ is notation for the event that the ith site is in the state C, this is equivalent to showing, in the case of arbitrary Γ that $\nu_\Gamma(-\mid C')\geqslant_{\text{FKG}}\nu_\Gamma(-\mid C)$. However, the weights defined by

$$W_\varepsilon(\alpha)=\begin{cases}\mu(\alpha) & \text{if } \alpha(i)=C \text{ or } C'\,,\\ \varepsilon\mu(\alpha) & \text{otherwise}\end{cases} \tag{B.13}$$

still satisfy the lattice condition. The event $\alpha(i) \leqslant C$ is decreasing and the event $\alpha(i) \geqslant C'$ is increasing. Calling the measure that result from the weights in Eq. (B.13) $\mu_\Gamma^e(-)$, and letting Φ denote any positive event, we have

$$\mu_\Gamma^e(H \mid \alpha(i) \geqslant C') \geqslant \mu_\Gamma^e(H) \geqslant \mu_\Gamma^e(H \mid \alpha(i) \leqslant C) . \tag{B.14}$$

and we get the dominance of $\mu_\Gamma(- \mid C'(i))$ over $\mu_\Gamma(- \mid C(i))$ by continuity. By "integrating down" (as in the first argument in this proof) we get the desired dominance for the ν's. The only unanswered claim is the strong FKG property for the measures $\nu_\Gamma(-)$, i.e. if $\# \in \{0,1\}^\Xi$ we need that $\nu_\Gamma(- \mid \#)$ is still FKG. Without loss of generality, we may consider the case where $\#$ consists only of 1's, i.e. by considering a smaller lattice.

Let us prove the statement by the following inductive scheme: We claim that for all finite lattices Γ, for all $\Xi \subset \Gamma$, for all boundary conditions $*$ on $\Gamma \backslash \Xi$ and for all $K \subset \Gamma$, the measures $\nu_\Xi^*(- \mid \zeta(K) \equiv 1)$ are FKG and satisfy

$$\nu_\Xi^*(- \mid \zeta(K) \equiv 1) \underset{\text{FKG}}{\leqslant} \nu_\Xi^{*\prime}(- \mid \zeta(K) \equiv 1)$$

if $* \prec *'$. This statement has evidently been demonstrated if $|K| = 0$. Assuming that this holds for $|K| = k$, let us add an additional site, say the site i to the set K: $\tilde{K} = K \cup \{i\}$.

Starting on the lattice $\Xi \backslash \{i\}$ consider the measures $\nu_\Xi^{*,A_i}(- \mid \zeta(K) \equiv 1), \ldots, \nu_\Xi^{*,D_i}(- \mid \zeta(K) \equiv 1)$ defined by fixing the value at the site i to be $A, \ldots, D$. By the inductive hypothesis, these measures are FKG and satisfy

$$\nu_\Xi^{*,A_i}(- \mid \zeta(K) \equiv 1) \underset{\text{FKG}}{\geqslant} \cdots \underset{\text{FKG}}{\geqslant} \nu_\Xi^{*,D_i}(- \mid \zeta(K) \equiv 1) . \tag{B.15}$$

Now the desired measure, $\nu_\Xi^*(- \mid \zeta(\tilde{K}) \equiv 1)$, is seen to be a convex combination of these measures. However (cf. [33, Proposition 2.22]) it is not difficult to show that the convex combination of FKG measures that have a definitive FKG ordering is itself an FKG measure. Thus we have that $\nu_\Xi^*(- \mid \zeta(\tilde{K}) \equiv 1)$ is FKG. We are not quite done because we still have to verify that if $*' \succ *$, then $\nu_\Xi^{*\prime}(- \mid \zeta(\tilde{K}) \equiv 1)$ FKG dominates $\nu_\Xi^*(- \mid \zeta(\tilde{K}) \equiv 1)$. However, we may establish this by raising the boundary values (of $*$) one at a time. In this case, the result may be obtained by pretty much the same technique that was used in the $|K| = 0$ case: Run through the whole procedure with an "unconditioned" measure that is concentrated on two values for the targeted site of $*$ and the desired dominance follows from the newly acquired FKG property. □

B.3. Back to multicolors

In this appendix, we reanalyze the orthodox region and beyond ($\Delta > 2$) from the perspective of the multicolored representation of Section 2. The principal motivation is to provide support for the reasonable picture that under *some* conditions of symmetry and ferromagnetic orthodoxy, (a) the grey reduction of the multicolored measure is FKG and (b) Ferromagnetism occurs if and only if there is percolation of blues. Partial results for (a) and (b) can be found for the four-state model outside the reformed

region. However, as an algorithmic tool, what follows is of limited use in its present form; the paper is self-contained without this appendix and the appendix should be omitted on a first reading.

Recalling that in the multicolored representations, some of the bonds are oriented, for simplicity, let us exploit the bi-partite nature of the lattice and point all bonds from the even to the odd sublattice. Our working notation will be as follows: blue bonds, as always, force the neighboring values of the spins into the same state and red$^{\pm}$ signifies that the odd partner differs from the even partner by ± 1. We still assume symmetry ($\mathscr{E}_{0,+1} = \mathscr{E}_{0,-1}$) so the two species of red bonds have the same *a priori* weights.

First, let us observe that in the orthodox region, there is a connection between the grey reduction of the multicolored measure and a different sort of reduction of the duplicated Ising representation featured in Section 3.3.

Proposition B.4. Consider the two layer measure $\nu^{AT}_{(2,2),P}(-)$ for the standard AT model with $p_\kappa = p_\tau = 1 - e^{-\beta(\Delta-1)}$ and $p_{\kappa\tau} = 1 - e^{-\beta(2-\Delta)}$ defined for the region $2 \geqslant \Delta \geqslant 1$ on the configurations $(\omega_\kappa, \omega_\tau, \omega_{\kappa\tau})$. Let $\mu^{G}_{\Delta;\beta}(-)$ be the grey measure reduced from the multicolored representation of this model as defined in Eq. (2.10). Define $\zeta = \omega_\kappa \vee \omega_\tau \vee \omega_{\kappa\tau}$, i.e. for each bond b, $\zeta(b) = 0$ if $\omega_\kappa(b) = \omega_\tau(b) = \omega_{\kappa\tau}(b) = 0$ but is one if any bond is "visible". Then $\mu^{G}_{\Delta;\beta}(-)$ is equal to the "visually" projected measure:

$$\mu^{G}_{\Delta;\beta}(\zeta) = \sum_{\omega:\omega_\kappa \vee \omega_\tau \vee \omega_{\kappa\tau} = \zeta} \nu^{AT}_{(2,2),P}(\omega)\,.$$

Proof. The easiest method is via Edwards–Sokal weights for the two measures. Let ζ denote a grey configuration and let $\bar{\zeta}(\zeta)$ denote a legitimate coloring of ζ by blue and red$^{\pm}$ bonds. Let $R_b = e^{\beta\Delta} - 1$ and $R_r = e^{\beta(\Delta-1)} - 1$ denote the fugacity factors for blue and red bonds. We may write the weights:

$$W(\bar{\zeta}) = \sum_{\underline{\sigma}} R_b^{N_b(\bar{\zeta})} R_r^{N_{r^-}(\bar{\zeta})} R_r^{N_{r^+}(\bar{\zeta})} \mathbf{D}(\underline{\sigma}, \bar{\zeta}) \tag{B.16}$$

where $\mathbf{D}(\underline{\sigma}, \bar{\zeta})$ is one if the bond and spin configuration are consistent and zero otherwise. (Note that if the old $\mathbf{D}(\bar{\zeta})$ is zero then $\mathbf{D}(\underline{\sigma}, \bar{\zeta})$ will vanish for all $\underline{\sigma}$.) It should be recalled that within each connected bond-cluster of a multicolored configuration $\bar{\zeta}$, the relative orientation of the spins is completely determined. In particular, if $\bar{\zeta}$ and $\bar{\zeta}'$ have the same bonds but a different coloring then $\mathbf{D}(\underline{\sigma}, \bar{\zeta})$ and $\mathbf{D}(\underline{\sigma}, \bar{\zeta}')$ cannot both be one for any spin configuration $\underline{\sigma}$.

Let $\Omega(\zeta)$ denote the set of all the configurations in the duplicated Ising representation that would contribute to ζ:

$$\Omega(\zeta) = \{\omega \mid \omega_\kappa \vee \omega_\tau \vee \omega_{\kappa\tau} = \zeta\} \tag{B.17}$$

and let us temporarily denote the visually projected measure as $\tilde{\mu}^{G}_{\Delta;\beta}$:

$$\tilde{\mu}^{G}_{\Delta;\beta} \propto \sum_{\omega \in \Omega(\zeta)} Y^{AT}_{(2,2),P}(\omega)\,. \tag{B.18a}$$

We now express the weights $Y^{AT}_{(2,2),P}$ in Edwards–Sokal form, using fugacities as opposed to Bernoulli prefactors:

$$\tilde{\mu}^G_{\Delta;\beta}(\zeta) \propto \sum_{\omega\in\Omega(\zeta)} R_r^{N(\omega_\kappa)} R_r^{N(\omega_\tau)} L^{N(\omega_{\kappa\tau})} \sum_{\underline{\sigma}} \Delta(\omega,\underline{\sigma}) \tag{B.18b}$$

where (as it happens) $p_\kappa/(1-p_\kappa) = R_r = p_\tau/(1-p_\tau)$, $L \equiv p_{\kappa\tau}/(1-p_{\kappa\tau}) = e^{\beta(2-\Delta)} - 1$ and $\Delta(\omega,\underline{\sigma})$ was defined in Eq. (3.27). We exchange the order of summations in Eq. (B.18b) and notice that each $\underline{\sigma}$ that has $\Delta(\omega,\underline{\sigma}) = 1$ for some $\omega\in\Omega(\zeta)$ uniquely determines a legitimate coloring of ζ; i.e. a $\bar{\zeta}(\zeta)$ such that $\mathbf{D}(\bar{\zeta},\underline{\sigma}) = 1$. We thus have

$$\tilde{\mu}^G_{\Delta;\beta}(\zeta) \propto \sum_{\bar{\zeta}(\zeta)} \sum_{\underline{\sigma}:\mathbf{D}(\bar{\zeta},\underline{\sigma})=1} \sum_{\omega\in\Omega(\zeta)} R_r^{N(\omega_\kappa)} R_r^{N(\omega_\tau)} L^{N(\omega_{\kappa\tau})} \Delta(\omega,\underline{\sigma}) . \tag{B.19}$$

Now for fixed $\underline{\sigma}$ (with $\mathbf{D}(\bar{\zeta},\underline{\sigma}) = 1$ for some $\bar{\zeta}$) we may calculate, bond by bond, the combined weight of all the $\omega\in\Omega(\zeta)$ for which $\Delta(\omega,\underline{\sigma}) = 1$. E.g. if a bond in $\bar{\zeta}$ is red$^+$, *something* on this bond is required from ω since $\omega\in\Omega(\zeta)$; depending on the value of $\underline{\sigma}$ at the even site, the required bond is a κ-bond with no τ-bond or the other way around. In any case, the result for every red$^+$ is a factor of R_r and similarly for all the red$^-$ bonds. On the other hand, if a bond in $\bar{\zeta}$ is blue then ω is allowed to be anything except completely empty on that bond. This yields a factor of $(R_r+1)(R_r+1)(L+1)-1 = R_b$. Hence, we arrive at

$$\begin{aligned}\tilde{\mu}^G_{\Delta;\beta}(\zeta) &\propto \sum_{\bar{\zeta}(\zeta)} \sum_{\underline{\sigma}:\mathbf{D}(\bar{\zeta},\underline{\sigma})=1} R_r^{N_r-(\bar{\zeta})} R_r^{N_r+(\bar{\zeta})} R_b^{N_b(\bar{\zeta})} \\ &= \sum_{\bar{\zeta}(\zeta)} W(\bar{\zeta}) \;\propto\; \mu^G_{\Delta;\beta}(\zeta) . \qquad \square\end{aligned} \tag{B.20}$$

An immediate and pleasing consequence is

Corollary. In the orthodox region, the grey measures enjoy the FKG property.

Proof. If $A = A(\zeta)$ is an increasing function, it is clear that $\tilde{A}(\omega) = A(\omega_\kappa \vee \omega_\tau \vee \omega_{\kappa\tau})$ is increasing. Now, in general, $\mu^G_{\Delta;\beta}(A) = \nu^{AT}_{(2,2),P}(\tilde{A})$. Thus, if A and B are both increasing, $\mu^G_{\Delta;\beta}(AB) = \nu^{AT}_{(2,2),P}(\tilde{A}\tilde{B}) \geqslant \nu^{AT}_{(2,2),P}(\tilde{A})\nu^{AT}_{(2,2),P}(\tilde{B}) = \mu^G_{\Delta;\beta}(A)\mu^G_{\Delta;\beta}(B)$. $\square$

For the general case, $\Delta \geqslant 1$, we have the following, incomplete result.

Proposition B.5. Consider any infinite volume multicolored measure for the AT model in the region $\Delta \geqslant 1$ that emerges as a limit of blue-wired stated corresponding to 0's at the boundary. Let $P^B_\infty(i)$ denote the (possibly subsequential) limiting probability that the site at i is connected to the boundary by a path of blue bonds and let $P^R_\infty(i)$ denote the limiting probability that i is connected to the boundary by all paths use at least one red bond. In the corresponding spin system, let $\rho_0(i)$, $\rho_{+1}(i)$, $\rho_{-1}(i)$ and $\rho_2(i)$ denote the probability of observing the spin-state 0, $+1$, -1 or 2 at the site i and

define the magnetization at i as $\vec{m}(i) = (\rho_0(i) - \rho_2(i), \rho_{+1}(i) - \rho_{-1}(i))$. Then, in this state, $\vec{m}(i) \neq 0$ iff $P^B_\infty(i) \neq 0$, i.e. there is positive magnetization in this state if and only if there is percolation of blue bonds. Furthermore, if there is no blue percolation in any limiting state, the spontaneous magnetization is zero.

Proof. We may consider the situation in finite volume and the desired conclusions will hold in the limiting state. If the site at i is disconnected from the boundary, the contribution to all four densities is equal and if the site is blue connected to the (blue wired) boundary, the contribution is exclusively to $\rho_0(i)$. Let $\overline{\omega}$ denote a (legitimate) configuration in which each path from i to the boundary goes through at least one red bond. Let $C_B(i)$ denote the set of sites that can be reached from i by a path that uses only blue bonds (which may consist of the site i alone). Now consider the collection of red bonds that connect a site in $C_B(i)$ to a site outside $C_B(i)$ and let $\overline{\omega}^\#(i)$ denote the configuration that is identical to $\overline{\omega}$ except that the above-mentioned red bonds have reversed signature: $\text{red}^+ \leftrightarrow \text{red}^-$. It is clear that if $\overline{\omega}$ is a legitimate configuration then so is $\overline{\omega}^\#(i)$. Indeed, any elementary loop either makes no use of these bonds or uses two of them as it passes in and out of $C_B(i)$. In the latter case, the oriented sum around the loop may change by four but this is equivalent to zero. It is also obvious by the $\text{red}^+/\text{red}^-$ symmetry that the probability of $\overline{\omega}^\#(i)$ is the same as the probability of $\overline{\omega}$. Now, with the identification of any fixed boundary condition in the spin system, it is not hard to see that if $\sigma_i(\overline{\omega}) = 0$ then $\sigma_i(\overline{\omega}^\#(i)) = 2$ and vice versa while if $\sigma_i(\overline{\omega}) = \pm 1$ then $\sigma_i(\overline{\omega}^\#(i)) = \mp 1$. Thus, in any boundary condition, the contribution of these configurations to $\vec{m}(i)$ is zero. So, if there is no blue percolation in any state, the spontaneous magnetization vanishes and furthermore, in the wired state, $\vec{m}(i)$ is exactly $(P^B_\infty(i), 0)$. □

Remark. For the region $\Delta > 2$, we must be content with Proposition B.5 as it stands. When $1 \leqslant \Delta \leqslant 2$, we know from the representation of Eq. (3.20) that blue-wired boundary conditions, which are equivalent to the usual wired boundary conditions in this representation, are exactly the ones that produce the spontaneous magnetization in the limiting state. Thus we have non-uniqueness if and only if we have blue percolation in the blue wired state. Presumably, the same holds if $\Delta > 2$ but a proof has eluded us. Furthermore, for any Δ, we cannot rule out the (absurd) possibility of blue percolation in some state but no blue percolation in the blue wired state.

References

[1] D. Kandel and E. Domany, Phys. Rev. B 43 (1991) 8539–8548.
[2] R.H. Swendsen and J.S. Wang, Phys. Rev. Lett. 58 (1987) 86.
[3] U. Wolff, Phys. Rev. Lett. 62 (1989) 361.
[4] R.G. Edwards and A.D. Sokal, Phys. Rev. D 38 (1988) 2009–2012.
[5] X.-J. Li and A.D. Sokal, Phys. Rev. Lett. 63 (1989) 827–830.
[6] U. Wolff, Phys. Rev. Lett. B 228 (1989) 379.
[7] J. Machta, Y.S. Choi, A. Lucke, T. Schweizer and L.V. Chayes, Phys. Rev. Lett. 75 (1995) 2792–2795.

[8] J. Machta, Y.S. Choi, A. Lucke, T. Schweizer and L.M. Chayes, Phys. Rev. E. 54 (1995) 1332–1345.
[9] D. Kim, P.M. Levy and F. Uffer, Phys. Rev. B 12 (1975) 989.
[10] E. Domany and E. Riedel, Phys. Rev. B 19 (1979) 5817–5834.
[11] C. Fan, Phys. Rev. B 6 (1972) 902.
[12] M. Aizenman, J.T. Chayes, L. Chayes and C.M. Newman, J. Stat. Phys. 50 (1988) 1–40.
[13] H.O. Georgii, Gibbs Measures and Phase Transitions (de Gruyter, New York, 1988).
[14] L. Onsager, Phys. Rev. 65 (1944) 117–149.
[15] M. Aizenman, D. Barsky and R. Fernandez, J. Stat. Phys. 47 (1987) 343–374.
[16] R. Kotecký and S.B. Shlosman, Comm. Math. Phys. 83 (1982) 493–515.
[17] R. Kotecký, L. Laanait, A. Messager and J. Ruiz, J. Stat. Phys. 58 (1990) 199.
[18] L. Laanait, A. Messager, S. Miracle-Sole, J. Ruiz and S. Shlosman, Comm. Math. Phys. 140 (1991) 81–91.
[19] L. Chayes, Private calculation.
The calculation is for the Bethe lattice with coordination number three. Let $R = e^{\beta} - 1$ and $\Delta = \mathscr{E}_{0,2} + 1$ and the lowest energy set to -1. The calculation takes place away from the Potts limit so there *is* an intermediate phase and no first-order transitions. Let θ be the order parameter for the intermediate phase. Then magnetization set in when

$$\frac{a(1 + b\theta)}{1 + b^2\theta^2} = 1$$

while percolation of blue bonds begins when

$$\frac{1}{2}\frac{R}{r}\frac{(1 + b\theta)}{1 + b^2\theta^2} = 1 .$$

In the preceding, $r = \frac{1}{4}e^{\beta}[1 + e^{-\beta\Delta}] + \frac{1}{2}$, $b = r^{-1}(\frac{1}{4}e^{\beta}[1 + e^{-\beta\Delta}] - \frac{1}{2})$ and $a = r^{-1}(\frac{1}{2}e^{\beta}[1 + e^{-\beta\Delta}])$. Thus, it is enough that $\frac{1}{2}R > ar$, i.e. $e^{\beta} - 1 > e^{\beta}(1 - e^{-\beta\Delta})$ which is satisfied whenever $\Delta < 1$.
[20] L. Chayes, Private calculation.
The result is as follows for coordination number of three: Let R and R_0 denote the quantities defined in the text. If the transition is second order (which is easily verified well away from the Potts limit) the percolation of combined red and blue occurs when $R = 4$ while magnetization sets in when $R_0 = 4 + 2R$, i.e. a strictly lower temperature.
[21] J. Ashkin and E. Teller, Phys. Rev. 64 (1943) 178–184.
[22] C.E. Pfister, J. Stat. Phys. 29 (1982) 113–116.
[23] F.J. Wegner, Teller and the eight vertex model, J. Phys. C 5 (1972) L131–L132.
[24] M. Campanino and L. Russo, Three-dimensional cubic lattice, Ann. Prob. 13 (1985) 478–491.
[25] L. Chayes, R. Kotecký and S. Shlosman, Dilute spin systems, Comm. Math. Phys. 171 (1995) 203–232.
[26] S. Sarbach and F.Y. Wu, Z Phys. B 44 (1981) 309.
[27] M. Aizenman, J.T. Chayes, L. Chayes and C.M. Newman, Ising and Potts ferromagnets, J. Phys. A 20 (1987) L313–L318.
[28] S. Wiseman and E. Domany, Phys. Rev. E 48 (1993) 4080–4090.
[29] M.P.M. den Nijs, Private communication.
[30] S.B. Shlosman, First-order phase transitions, Russian Math. Surveys 41(3) (1986) 83–134.
[31] M. Biskup, L. Chayes and R.Kotecký, in preparation.
[32] C. Borgs, R. Kotecký and S. Miracle-Solé, J. Stat. Phys. 62 (1991) 529–551.
[33] T.M. Liggett, Interacting Particle Systems (Springer, Heidelberg, 1985).